STUDIES ON REMOVAL OF SELENIUM FROM WATER BY ADSORPTION

A DISSERTATION

Submitted in partial fulfillment of the requirements for the award of the degree of

MASTER OF TECHNOLOGY

in

CHEMICAL ENGINEERING

(With Specialization in Industrial Pollution Abatement)

By

CH SEKHARARAO GULIPALLI

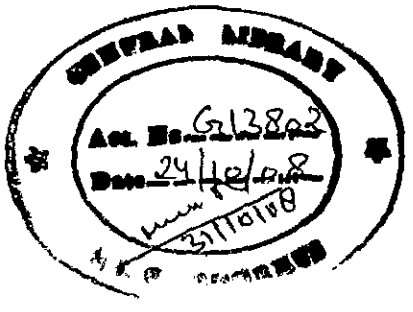

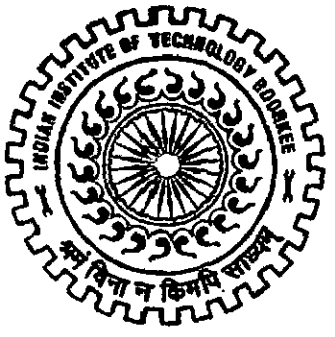

DEPARTMENT OF CHEMICAL ENGINEERING
INDIAN INSTITUTE OF TECHNOLOGY ROORKEE
ROORKEE - 247 667 (INDIA)

JUNE, 2008

INDIAN INSTITUTE OF TECHNOLOGY ROORKEE
ROORKEE

CANDIDATE'S DECLARATION

I hereby certify that the work which is being presented in the dissertation entitled **STUDIES ON REMOVAL OF SELENIUM FROM WATER BY ADSORPTION** in partial fulfilment of the requirements for the award of the degree **Master of Technology** with specialization in **INDUSTRIAL POLLUTION ABATEMENT,** to the **Department of Chemical Engineering, Indian Institute of Technology Roorkee, Roorkee** is an authentic record of my own work carried out during a period from July 2007 to June 2008 under the supervision of Dr. B. Prasad, Associate Professor, Chemical Engineering Department, Indian Institute of Technology Roorkee, Roorkee.

The matter presented in this work has not been submitted by me for the award of any other degree of this or any other Institute.

Date: 27/06/08
Place: IIT, Roorkee

(CH SEKHARARAO GULIPALLI)

This is to certify that the above statement made by the candidate is correct to the best of our knowledge.

Dr. B. Prasad,
Associate Professor,
Department of Chemical Engineering,
Indian Institute of Technology Roorkee,
Roorkee, Uttarakhand (India).

ABSTRACT

The present work involves the study of Se(IV) adsorption onto bagasse fly ash (BFA), rice husk ash (RHA), granular activated carbon (GAC) and powdered activated carbon (PAC). The adsorbents were coated with the ferric chloride solution for the effective removal. The physico-chemical characterization of the adsorbents has been carried out using standard methods e.g. proximate analysis, scanning electron microscopy (SEM), fourier transform infrared spectroscopy (FTIR), thermo-gravimetric (TGA) and differential thermal analysis (DTA), etc.

Batch experiments were carried out to determine the effect of various factors such as adsorbent dose (w), initial pH, contact time (t), and temperature (T) on adsorption process. Results obtained from these studies have been analyzed by various kinetic models and isotherms. From the results it has been inferred that PAC is having highest removal efficiency among all the adsorbents used at natural pH. Se(IV) adsorption onto all the adsorbents used is high at low pH values, and decreased with the rise in initial pH. Temperature study shows that the uptake of Se(IV) by all adsorbents is more at 293 K with in the temperature range studied. The parameters of Pseudo-First order, Pseudo-Second order kinetics, Weber-Morris intra particle kinetics have been determined. Equilibrium isotherms have been analyzed using Langmuir isotherm, Freundlich isotherm and Temkin isotherm and parameters have been calculated for all the isotherms. Error analysis has also been done using hybrid fractional error function (HYBRID) and Marquardt's percent standard deviation (MPSD).

ACKNOWLEDGEMENTS

I express my deep sense of gratitude to Dr. B. Prasad, Associate Professor, Department of Chemical Engineering, Indian Institute of Technology Roorkee, Roorkee, for his precious guidance, suggestions and supervision at every level of my dissertation. I am obliged forever for his kind inspiration, encouragement and wholehearted support without which it was not possible to complete my work.

I would like to take this opportunity to put on record my respects to Prof. Shri Chand, Head of the Department, for providing me various facilities during the course of the present work. My sincere and grateful thanks are also due to Prof. I.M. Mishra, Prof. Surendra Kumar and Prof. I.D. Mall, Department of Chemical Engineering, IIT, Roorkee for their kind assistance and encouragement.

I would like to thank specially to Dr. Vimal Chandra Srivastava, for his generous help during my work.

I am thankful to Prof. Kailash Chandra, and Prof. A. K. Chaudhary of the Institute Instrumentation Centre for their generous assistance and facilitation in the analysis of the samples.

Special thanks are due to technical staff of the Department; Shri Ayodhya Prasad Singh, Shri. Rajendra Bhatnagar, Shri Tara Chand and Shri H. Anda of the Institute Instrumentation Centre for helping me during the course of my experimental work.

I do not have enough words to thank all my friends who encouraged and helped me to complete this work at the earliest.

Above all, I would like to acknowledge that the greatest was played by my parents who kept their pleasures away to educate me and who cultivated the system of values and instincts that shall enlighten my path for the life time.

CH SEKHARARAO GULIPALLI

CONTENTS

LIST OF FIGURES

LIST OF TABLES

ABBREVIATIONS AND NOTATIONS

ABBREVIATIONS

BFA	Bagasse fly ash
CPCB	Central pollution control board
DTA	Differential thermal analysis
DTG	Differential thermal gravimetery
EDAX	Energy dispersive X-ray analysis
FTIR	Fourier transform infrared spectroscopy
GAC	Granular activated carbon
HYBRID	Hybrid fractional error function
ICPMS	Inductively coupled plasma mass spectroscopy
MPSD	Marquardt's percent standard deviation
PAC	Powder activated carbon
RHA	Rice husk ash
SEM	Scanning electron microscopy
TG	Thermal gravimetery
TGA	Thermo-gravimetric analysis
UNICEF	United Nations International Children's Emergency Fund
US EPA	United States Environmental Protection Agency

NOTATIONS

C_o	Initial concentration of adsorbate in solution, μg/l
C_e	Equilibrium liquid phase concentration, μg/l
C_t	Equilibrium liquid phase concentration after time t, μg/l
q_e	Equilibrium adsorption capacity, μg/g

q_t	Equilibrium adsorption capacity after time t, μg/g
k_s	Pseudo-second-order rate constant, g/μg.min
h	Initial sorption rate, μg/g.min
k_f	Pseudo 1st order rate constant, min^{-1}
K_{id}	Intra-particle diffusion rate constant, μg/g min$^{1/2}$
I	Constant that gives idea about the thickness of boundary layer, μg/g
K_F	Freundlich constant, l/μg
$1/n$	Mono-component (non-competitive) Freundlich heterogeneity factor of the single component, dimensionless
K_L	Langmuir adsorption constant, l/μg
B_T	Temkin Isotherm constant, related to the heat of adsorption
b	Temkin Isotherm constant
t	Time, min
V	Volume of the solution, l
w	Mass of the adsorbent, g/l
R^2	Correlation coefficients
k	Rate constant, min^{-1}
R	Universal gas constant, 8.314 J/mol K
T_{max}	DTG peak temperature, K
T_{1i}	DTA first initial temperature, K
T_{2f}	DTA second final temperature, K

Chapter – I

INTRODUCTION

1.1 GENERAL

Water is a common chemical substance that is essential for the survival of all known forms of life. Water fit for human consumption is called drinking water or potable water. Currently, about 1 billion people around the world routinely drink unhealthy water. Poor water quality and bad sanitation are deadly; some 5 million deaths a year are caused by polluted drinking water. Water, however, is not a finite resource (like petroleum is), but rather re-circulated as potable water in precipitation in quantities many degrees of magnitude higher than human consumption. Therefore, it is the relatively small quantity of water in reserve in the earth (about 1% of our drinking water supply, which is replenished in aquifers around every 1 to 10 years), that is a non-renewable resource, and it is, rather, the distribution of potable and irrigation water which is scarce, rather than the actual amount of it that exists on the earth. Organizations concerned in water protection include International Water Association (IWA), Water Aid, Water 1st, American Water Resources Association. Water related conventions are United Nations Convention to Combat Desertification (UNCCD), International Convention for the Prevention of Pollution from Ships, United Nations Convention on the Law of the Sea and Ramsar Convention [Wikipedia].

In 1990, the challenge of ensuring universal access to safe drinking water by 2000 meant reaching 1.2 billion people, or 23 per cent of the world's population, with clean, sustainable water supplies. This challenge remained despite the gains made during the International Drinking Water Supply and Sanitation Decade (1981-1990). According to UNICEF census in the year 2000, 1.1 billion people are still without access to safe drinking water and percentage contribution of the various parts of the world is shown in Table 1.1.1. the comparison of the percentage of population without access to safe drinking water in the Asian continent. is shown in Table 1.1.2

Table 1.1.1. Percent of population without access to drinking water in various parts of the world (Total = 1.1 billion)

Region	Percent of population without access to safe drinking water
Middle-East/North Africa	4%
Latin America/Caribean	6%
South Asia	19%
Sub-Saharan Africa	25%
East Asia/Pacific	42%

Table 1.1.2 Percent of population without access to safe drinking water

Country	Per cent of population with out access to safe drinking water	
	1990	2000
Bangladesh	6	3
Pakistan	17	10
Nepal	33	12
India	32	16
Sri Lanka	32	23
Bhutan	-	38
Afghanistan	-	87

Contamination of selenium in ground waters has attracted worldwide attention. Although it is an essential element for animal and human nutrition, in high concentrations it has been shown to create toxicity problems in livestock and wildlife. Because of its high toxicity, the US EPA has proposed a standard of 0.05 mg/l for drinking water. For inland surface water, public sewers and marine/coastal areas, the Central Pollution Control Board (CPCB), Delhi, India has set a standard of 0.05 mg/l.

1.2 SELENIUM

Selenium is a semi-metallic element with atomic number 34 and an atomic mass of 78.96. It belongs to Group VIA of the periodic table, located between sulfur and tellurium, and resembles sulfur both in its various forms and in its compounds. Selenium exists in several allotropic forms. The stable form at ordinary room temperatures is the grey or hexagonal form with a melting point of 220.5 ^{0}C . The other two important forms are red (monoclinic) with a melting point of 221 ^{0}C and amorphous selenium, which exists in black and red forms. Black amorphous selenium is vitreous and is formed by the rapid cooling of liquid selenium. Red amorphous selenium is colloidal and is formed in reduction reactions . Physical properties of selenium and sodium selenite are presented in Table 1.2.1.

The chemical properties of selenium are similar to sulfur. Selenium combines with metals and many non metals directly or in aqueous solution. The selenides resemble sulfides in appearance, composition, and properties. Selenium may form halides by reacting vigorously with fluorine and chlorine, but the reactions with bromine and iodide are not as rapid. Selenium does not react directly with hydrogen fluoride or hydrogen chloride, but decomposes hydrogen iodide to liberate iodine and yield hydrogen selenide Selenium reacts with oxygen to form a number of oxides, the most stable of which is selenium dioxide.

Selenium can exist in four oxidation states in the environment: selenite (Se(IV)), selenate (Se(VI)), elemental selenium (Se(0)) and selenide (Se(II)). These oxidation states can be found in particles and sediments; therefore, seleniteand and selenate can either be adsorbed onto particles or exist as metal selenites or selenates. Selenides can be found as inorganic selenides, usually FeSe (achavalite) or $FeSe_2$(ferroselite), or as organic forms such as selenoaminoacids. These particles act as an elemental reservoir and may release the different chemical forms of the element into natural water (river, estuary or sea) through an adsorption/desorption process that has been extensively studied [Camara et al., 1995].

Se(IV) and Se(VI) are both water soluble inorganic species commonly found in aerobic water sources and elemental Se is more readily found in anaerobic sediments.

Table1.2.1:Physical properties of Selenium and Sodiumselenite

Property	**Selenium**	**Sodium selenite**
Molecular weight	78.96	172.94
Color/form	Red, grey, or black	White tetragonal crystals
Physical state	Solid	Solid
Melting point	221 ^{0}C(red); 220.5 ^{0}C (grey); 180 ^{0}C (black)	
Boiling point	685 ^{0}C	
Density (g/cm^3)	4.39 (red); 4.81(grey); 4.28 (black)	
Odor	Unknown; upon combustion, smells like rotten horseradish	
Solubility: Water	Insoluble	Freely soluble in water
Vapor pressure	1 mmHg at 356 ^{0}C (grey)	
Heat of fusion	(gray) 6.69kJ.mol^{-1}	
Heat of vaporization	95.48 kJ. mol^{-1}	
Heat capacity	25.363 J. mol^{-1} K^{-1}	

Table 1.2.2 Health Hazard Information

Inhalation reference exposure level	20μg/m^3
Oral reference exposure level	0.005 mg/kg/day
Critical effects	Clininical selenosis
Hazard index targets	Alimentary system, cardiovascular system, nervous system

Se also forms into selenoproteins, such as selenomethionine, analogous to the essential amino acid methionine, in which sulfur is replaced by selenium.

Toxic effects of inorganic and organic Se are caused by the alteration of protein three dimensional structures and the impairment of enzymatic function of an organism. Health hazard information of selenium is given in Table 1.2.2.

1.2.4 Sources of Selenium

The introduction of selenium in the environment by anthropogenic activities is derived by agricultural irrigation drain water, mining activities and industrial effluent discharge, including oil refinery effluents.

Selenium is most commonly produced from selenide in many sulfide ores such as those of copper, silver, or lead. It is obtained as a byproduct of the processing of these ores, from the anode from the anode mud of copper refineries, and the mud from the lead chambers sulfuric acid plants. These muds can be processed by a number of means to obtain free selenium. Natural sources of selenium include certain selenium-rich soils, and selenium that has been bioconcentrated by certain toxic plants such as lowceed. Anthropogenic sources of selenium include coal burning and the mining and smelting of sulfide ores.

Selenium contamination originates from many sources including mining operations, mineral processing operations, abandoned mine sites, petroleum processing, agricultural runoff and natural groundwater. For mining waste, the principal sources of selenium contamination are copper- and uranium-bearing ores and sulfur deposits. Selenium is commonly found in mining wastewaters in concentrations ranging from 3 to >12,000 µg/l.

1.2.3 Applications

Selenium compounds are widely used in glass manufacture, electronic applications, photocopy machines, inorganic pigments, rubbers, ceramics, plastics, lubricants, etc. Indusrial uses of selenium compounds are summarized in Table 1.2.3. [Camara et al., 1995]

Table 1.2.3 Industrial uses of different Se compounds

Compound	Uses
Selenium	Solar batteries, photoelectric cells, xerography, stainless steel
Na_2SeO_4	Insecticide, veterinary agent, glass manufacture
Na_2SeO_3	Veterinary agent, glass manufacture, soil additive
Selenium diethyl dithio carbamate	Fungicide
SeS_2	Veterinary agent, shampoos, semiconductors
SeS	Veterinary agent, fungal infections, eczema
SeF_6	Gaseous electric insulator
$SeOCl_2$	Solvent
$CuSeO_4$	Copper alloys
WSe_2	Lubricants
Al_2Se_3, Bi_2Se_3, CuSe, InSe	Semiconductors
$(NH_4)SeO_3$, As_2Se	Manufacture of red glass
CdSe	Photoconductors, semiconductors, photoelectric cells, solar batteries

1.2.5 Scope of the Problem

In India several incidents of chronic selenium toxicity in animals have been reported [Subramanian, 2001]. Selenium poisoning in domestic buffaloes in the Karnal area of the north west plain of India has been reported. High selenium levels found in the animals are attributed to the readily available selenium in the alkaline soils of the regions. Selenium is leached from the soil by irrigation water in the paddy fields and is taken up by rice plants, which accumulates it to toxic levels in the straw. This is the main fodder of the animals after harvest and is immediate cause of the toxicity. A similar pattern of mobilization of naturally occurring selenium caused by paddy field irrigation that also resulted in poisoning of domestic animals was reported from southern India.

In Enchi province in China, where the worst outbreaks of human selenosis have been recorded, while the sources of the poisoning was the highly recorded, while the source of the poisoning was the hihly seleniferous seams of coal from which the element was leached by weathering, a number of human activities contributed significantly to the epidemics. The traditional use of lime fertliser made the selenium accumulated in soil more readily available. More over, because of drought and the consequent failure of their rice crop, villagers consumed more than their usual intakes of vegetables and maize, which accumulate more selenium than dose rice. Plant ash, mase from the selenium-enriched maize straw, was also used in quantity as a crop treatment. In addition to all such enhancements of dietary levels of selenium, burning of local coal for coking and heating also probably contributed to selenium contamination of the air and of foods. In drought-free years of plenty, when locals consumed other foods and their protein intake in particular was increased, selenium intake was not a serious problem, even though natural levels in the environment were high.

Selenium is a problem in many wastewaters and is a common water contaminant throughout the world. Selenium contamination represents a major environmental problem in at least nine western U.S.states [EPA/600/R-01/077; 2001].

1.3 SELENIUM REMOVAL TECHNOLOGIES

There are several methods available for removal of selenium from water in large conventional treatment plants. These include adsorption by ferrihydrite, catalyzed cementation, biological reduction, enzymatic reduction etc.. Some of the studies for the removal of selenium from water and waste water are given in Table 1.3.1.

Table1.3.1. Treatment methods for the removal of selenium from water and waste waters

Treatment method	Component	Adsorbent/strain	Reference
Adsorbtion	Se(IV)	Sulphuric acid-treated peanut shell	Shafey [2007a]
Sorption	Se(IV), Se(VI)	Iron oxides	Miquel et al. [2007]
Sorption	Cd(II), Se(IV)	Modified rice husk	Shafey [2007b]
Adsorbtion	Se(IV), Se(VI)	Hydrous aluminum oxide (HAO) and corundum (α-Al_2O_3)	Derek [2006]
Adsorbtion	Se(IV)	Organic carbon coated sand	Yiqiang et al. [2005]
Adsorbtion	Se(IV), Se(VI)	Cs-covered Si(100) 2 x 1 surfaces	Sotiropoulos et al. [2003]
Adsorbtion	Se(IV), Se(VI)	Mg–Al and Zn–Al layered double hydroxides	Youwen et al. [2001].
Ferrihydrite adsorption	Se(VI)	Ferrihydrite	(EPA/600/R-01/077)
Catalyzed cementation	Se(IV), Se(VI), As, thallium	Iron	(EPA/600/R-01/077)
Biological reduction of selenium	Se(IV), Se(VI)	By developing bio films.	(EPA/600/R-01/077)
Enzymatic reduction	Se(IV), Se(VI)	Bacterial enzymes	(EPA/600/R-01/077)
Adsorbtion	Se(IV), Se(VI)	GaAs(111)A–(2x2)surface	Akihiro et al.[2000]
Adsorbtion-desorption	Se(IV), Se(VI)	Acidic and alkaline soils	Dhillon. [1999]
Adsorbtion	Se(IV), Se(VI)	Aluminum-oxide-coated sand (AOCS)	Wen-hui kuan et al. [1997]
Adsorbtion	Se(IV), Se(VI)	Iron oxyhydroxide and manganese dioxide	Laurie et al.[1990]

1.4 BAGGASE FLY ASH AND RICE HUSK ASH AS ADSORBENTS

1.4.1 BFA

Large quantities of industrial by-products are produced every year by chemical and agricultural process industries in India. These materials pose problems of disposal and their management, and also health hazards. However, some of these agricultural wastes have been found to be good adsorbents for the treatment of wastewaters and industrial effluents. BFA has been used by many researchers as an adsorbent for the removal of various metals and other chemicals from the wastewaters. RHA as agri-based waste material available free of cost from the particulate removal equipment attached to the boiler furnaces using rice husk as the fuel, has been shown to have high adsorption efficiency for the removal of cadmium (Cd(II)), nickel (Ni(II)) and zinc (Zn(II)) metal ions, lead and mercury.

A number of low-cost alternative adsorbents have been limited in their use. The surface area of most of the alternative adsorbents has been found to be low resulting in poor adsorptive capacity. The comparative studies on the adsorption of different adsorbents have not been carried out. However, the development of low-cost adsorbents with good surface area, exhibiting good adsorption potential for the removal of toxic compounds from wastewater is an important area.

BFA is a waste material formed during the combustion of bagasse, as a fuel in the boilers of the sugar mills. BFA is also obtained from particulate collection equipment connected to bagasse-fired boilers and emission stacks on the upstream and downstream sides, respectively. About 10 million tonnes of bagasse is produced annually in India. About 90% of this bagasse is used as a fuel in bagasse fired boilers. The production of bagasse fly ash is estimated to be about 3 kg/tonne of sugar produced. With the overall bagasse fly ash collection efficiency of 80% in the dust collection equipment, it is estimated that fly ash availability from the sugar industry would be of the order of 0.5 million tonnes/year [Kumar, 2007].

The adsorption properties of BFA are highly influenced with the firing practices of bagasse. Several investigators have recently shown interest in the use of bagasse fly ash as an adsorbent. It has been used for the COD removal from sugar mill, and paper

mill effluents. BFA has also been used for the adsorptive removal of phenolic compounds and dyes [Mall et al., 2005].

1.4.2 RHA

Rice husk is generally used for burning process. Rice mills and other rural area based industries use it as a fuel in their boilers/furnaces. Some rice mills also use it as a fuel to produce producer gas. It is a low cost adsorbent which has been used for the removal of pyridine and its derivatives [Lataye. et al., 2008].

The annual production of paddy rice globally was 579,500,000 tonnes in 2002. Rice is grown on every continent except Antarctica, over an area that covers about 1% of the earth's surface. It is a primary source of food for billions of people, and ranks second to wheat in terms of area and production Most paddy is produced by China (31%) followed by India (21%). During the milling process of paddy, rice husk is dehulled and removed. Thus the rice husk is an agricultural waste, accounting for about one-fifth of the annual gross rice production about 545 million tons, in the world. Rice husk can be used for energy production and the production of activated carbon, silicon carbide and portland cement. Rice husk ash (RHA) is generally collected from the particulate-collection equipment attached upstream of flue gas stacks. Roughly about 15-18% of the mass of the husk is collected as RHA in the particulate collection equipment. [Lataye, 2007].

RHA has many applications due to its attractive properties. It is an excellent insulator, so has applications in industrial processes such as steel foundries, and in the manufacture of insulation for houses and refractory bricks. RHA has also been used in the production of sodium silicate films. Since the main components of rice husk are carbon and silica, it has the potential to be used as an adsorbent as well. RHA has been used for the removal of metals [Srivastava et al., 2006].

1.5 OBJECTIVES OF THE PRESENT STUDY

The objectives of the present study are.

1. To characterize agri-based waste materials like bagasse fly ash (BFA), and rice husk ash (RHA) and the two types of activated carbons viz., granular (GAC) and- powdered(PAC) for their physico-chemical and adsorption properties. These characteristics include the proximate analysis and the surface and functional characteristics by FTIR, EDAX and SEM analyses.
2. To use BFA RHA, GAC and PAC as adsorbents for the treatment of the selenium bearing waters.
3. To study the effect of various parameters like initial pH (pH_0), adsorbent dose (m), contact time (t), initial concentration (C_0), and temperature (T) on the removal of Se(IV) from the aqueous solution in batch study.
4. To study the kinetic and equilibrium adsorption and studies for the adsorption of Se(IV) onto all adsorbents and to analyze the experimental data using various kinetic and isotherm models.
5. To understand the thermal degradation of spent adsorbents using TGA and DTG techniques.

Chapter-II

LITERATURE REVIEW

2.1 GENERAL

This chapter has been divided into tow parts: the first part deals with review of various studies on the removal of selenium from water and waste waters. In the second part, a comprehensive review of literature on the removal of various types of adsorbates from aqueous solutions by adsorption using bagasse fly ash (BFA), rice husk ash (RHA) , granular and powdered activated carbons (GAC and PAC), has been reported.

2.2 TREATMENT METHODS FOR SELENIUM

Adsorption of selenium by amorphous iron oxyhydroxide and manganese dioxide was studied by Laurie et al. [1990]. This work compares and models the adsorption of selenium and other anions on a neutral to alkaline surface (amorphous iron oxyhydroxide) and an acidic surface (manganese dioxide). Selenium adsorption on these oxides is examined as a function of pH, particle concentration, oxidation state, and competing anion concentration in order to assess how these factors might influence the mobility of selenium in the environment.

Adsorption voltammetry of selenium in the presence of phenylenediamine (*o*-PDA) was studied by Jinggyan et al. [1990]. The adsorptive voltammetric behaviour of Se(IV) on the HMDE in the presence of *o*-PDA has been investigated. Experimental results show that the Se (IV) complex with *o*-PDA can be adsorbed on the surface of the HMDE, yielding two peaks at -0.13 V and -0.62 V corresponding to the reduction of both the Se(N) complex and the Se(O) complex with *o*-PDA adsorbed on the surface of the HMDE. The mechanism of the reaction has also been described by them.

Removal of Se(IV) and Se(VI) by using Aluminum-Oxide-Coated sand (AOCS) was studied by Wen-hui kuan et al. [1997]. AOCS was evaluated for the removal of Se(IV) and Se(VI) from water. Quartz sand was coated at 70^0 C using 1M $AlCl_3$ solution

aging for 2 d at various coating pH ($pH_{(coating)}$). The Al oxide coating was an X-ray noncrystalline, porous compound at low $pH_{(coating)}$, while at high $pH_{(coating)}$, the AOCS could beter withstand acid/alkali and the coatings tented to form crystalline boehmite and bayerite. Adsorption of Se(IV) and Se(VI) was more effective using sand coated at low $pH_{(coating)}$ than at high $pH_{(coating)}$ AOCS produced at $pH_{(coating)}$ 5.98 had optimum properties and was employed as adsorbent. Adsorption experiments of Se(IV) and Se(VI) by AOCS peformed as a function of pH, initial concentration, reaction time and competing ion concentrations were examined. Removal of Se(IV) and Se(VI) increased with decreasing pH but greater for Se(IV) than Se(VI). In Se(IV) and Se(VI) mixed systems, the adsorption of Se(IV) was inhibited by Se(VI) oly at system pH ranging from 3 to 8 and the degree of inhibition was similar at Se(IV) to Se(VI) molar ratios of 1 and 3. However Se(VI) adsorption significantly decreased with with increasing Se(IV) concentration at all system pH. The sequence of foreign anions competing with respect to Se(IV) and Se(VI) adsorption was in order of $SO_4^{2-} > HCO_3^-$.

Adsorption–desorption reactions of selenium in some soils of India was investigated by Dhillon et al.[1999] at Department of Soil, Punjab Agricultural University in laboratory studies for surface soil samples varying in physico-chemical characteristics and mineralogical composition. In general, greater amount of Se was sorbed by acidic soils than alkaline soils; the only exception was the alkaline seleniferous soil from Barwa in northwestern India. Adsorption data for Se fitted well to Freundlich isotherm. Selenium adsorption data also conformed to Langmuir isotherm. Adsorption maxima was significantly correlated with organic carbon and free iron content of the soils.The distribution coefficient K_d showed that at the same value of surface coverage, the acidic soils had greater affinity for selenium as compared to the alkaline soils.

Selenium adsorption on Mg-Al and Zn-Al layered double hydroxides (LDHs) was studied by Youwen et al. [2000]. Layered double hydroxides LDHs have high anion exchange capacities that enhances their potential to remove anionic contaminants from aqueous systems. In this study, different Mg–Al and Zn–Al LDHs were synthesized by a coprecipitation method, with the products evaluated for their ability to adsorb selenite (SeO_3^{2-})nd selenate (SeO_4^{2-}). Results indicated the adsorption isotherm for SeO_3^{2-} retention by Mg–Al and Zn–Al LDHs could be fitted to a simple Langmuir equation with

the affinity of SeO_3^{2-} on Zn–Al LDH higher than that on Mg–Al LDH. The adsorption trends for both SeO_3^{2-} and SeO_4^{2-} on LDHs were similar under the experimental conditions. The SeO_3^{2-} adsorption was rapid and was affected by the initial SeO_3^{2-} concentration. The quasi-equilibrium for 0.063 and 0.63 cmol/l SeO_3^{2-} solutions was obtained within the first 30 and 60 min of adsorption, respectively. The maximum adsorption of SeO_3^{2-} on Mg–Al LDH was higher than that of Zn–Al LDH and decreased with an increase in the LDH mole ratio of Mg/Al. The high pH buffering capacities and the SeO_3^{2-} adsorption for Mg–Al and Zn–Al LDHs was a function of pH. Competing anions strongly affected the adsorption behavior of SeO_3^{2-} with SeO_3^{2-} adsorption increasing in the order: $HPO_4^{2-} < SO_4^{2-} < CO_3^{2-} < NO_3^-$. The release of adsorbed SeO_3^{2-} depended upon the type of competing anion in the aqueous solution.

Akihiro et al. [2000] studied adsorption processes of Se on the GaAs (111) A–(2x2) surface was studied . The adsorption processes of Se on the GaAs (111) A surface have been systematically studied using reflection high-energy electron diffraction (RHEED), scanning tunneling microscopy (STM) , X-ray photoelectron spectroscopy (XPS), and total-reflection-angle X-ray spectroscopy (TRAXS). They have found that a reconstructed structure of $(2\sqrt{3} \times 2\sqrt{3})$ –$R30^0$ is formed on the Se-adsorbed GaAs (111) A. A structure model has been proposed for the GaAs (111) A– $(2\sqrt{3} \times 2\sqrt{3})$ – $R30^0$–Se surface, which consists of two Se trimers located at a hollow site of the GaAs (111) A surface and three Ga vacancies per unit cell. The proposed structure model sufficiently explains experimental data from RHEED, XPS, and STM, and satisfies electron counting requirements.

Selenium adsorption on Cs-covered Si(100) 2 x 1 surfaces was studied by Sotiropoulos and Kamaratos [2003] In this study of Se adsorption on caesiated Si(100) 2 x 1 surfaces in ultra high vacuum (UHV) using low energy electron diffraction, auger electron spectroscopy, thermal desorption spectroscopy and work function measurements. Selenium atoms on Cs/Si(100) 2 x 1 surface adsorb initially on uncaesiated portions of Si and subsequently on the Cs overlayer. The presence of Se increases the binding energy of Cs on Si(100). For Cs and Se coverages above 0.5 ml CsSe and $Cs_xSe_ySi_z$, compound formation was observed. The coadsorption of Se and Cs induces a high degree of surface disorder, while desorption most probably causes surface etching. The presence of Cs on

Si(100) 2 x 1 surfaces prevents the diffusion of Se into the Si substrate and greatly suppresses the formation of SiSe2 and SiSe3, detected when Se is adsorbed on clean Si(100) 2 x 1 surfaces.

Removal of selenium and arsenic by animal biopolymers was studied by Shin-Ichi Ishikaw et al.[2004]. The animal biopolymers prepared from hen eggshell membrane and broiler chicken feathers, which are byproducts of the poultry-processing industry, were evaluated for the removal of the oxyanions selenium [Se(IV) and Se(VI)] and arsenic [As(III) and As(V)] from aqueous solutions. The biopolymers were found to be effective at removing Se(VI) from solution. Optimal Se(IV) and Se(VI) removal was achieved at pH 2.5–3.5.. Se(VI) and As(V) sorption isotherms were developed at optimal conditions and sorption equilibrium data fitted the Langmuir isotherm model.

Kadriye saygi et al. [2006] studied speciation of selenium(IV) and selenium(VI) in environmental samples by the combination of graphite furnace atomic absorption spectrometric determination and solid phase extraction. A simple solid phase extraction procedure for speciation of selenium(IV) and selenium(VI) in environmental samples has been proposed prior to graphite furnace atomic absorption spectrometry. The method is based on the solid phase extraction of the selenium(IV)–ammonium pyrrolidine dithiocarbamate (APDC) chelate. After reduction of Se(VI) by heating the samples in the microwave oven with 4 mol l^{-1} HCl, the system was applied to the total selenium. Se(VI) was calculated as the difference between the total selenium content and Se(IV) content. The experimental parameters, pH, amounts of reagents, eluent type and sample volume were optimized. The recoveries of analytes were found greater than 95%. No appreciable matrix effects were observed. The adsorption capacity of sorbent was 5.20 mg g^{-1} Se (IV). The detection limit of Se (IV) (3sigma, n = 11) is 0.010_g l^{-1}. The preconcentration factor for the presented system was 100. The proposed method was applied to the speciation of selenium(IV), selenium(VI) and determination of total selenium in natural waters and microwave digested soil, garlic, onion, rice, wheat and hazelnut samples harvested various locations in Turkey with satisfactory results.. The relative errors and relative standard deviations were below 6 and 10%, respectively.

Adsorption mechanisms of selenium oxyanions at the aluminum oxide/water interface was studied by Derek et al.[2006]. Sorption processes at the mineral/water

interface typically control the mobility and bioaccessibility of many inorganic contaminants such as oxyanions. They have studied the bonding mechanisms of selenate (SeO_4^{2-}) and selenite (SeO_3^{2-}) on hydrous aluminum oxide (HAO) over a wide range of reaction pH using extended X-ray absorption fine structure spectroscopy. Additionally, selenate adsorption on corundum (α-Al_2O_3) was studied to determine if adsorption mechanisms change as the aluminum oxide surface structure changes. The overall findings were that selenite forms a mixture of outer-sphere and inner-sphere bidentate-binuclear (corner-sharing) surface complexes on HAO, selenate forms primarily outer-sphere surface complexes on HAO, and on corundum selenate forms outer-sphere surface complexes at pH 3.5 but inner-sphere monodentate surface complexes at pH 4.5 and above.. The results are consistent with a structure-based reactivity for metal oxides, wherein hydrous metal oxides form outer-sphere complexes with sulfate and selenate, but inner-sphere monodentate surface complexes are formed between sulfate and selenate and α-Me_2O_3.

Removal of Se(IV) from aqueous solution using sulphuric acid-treated peanut shell was studied by Shafey [2007]. A carbonaceous sorbent was prepared from peanut shell via sulphuric acid treatment. Se(IV) removal from aqueous solution on the sorbent was studied varying time, pH, Se(IV) concentration, temperature and sorbent status (wet and dry). Se(IV) removal was faster using the wet sorbent than the dry sorbent following a pseudo-first-order model. Se(IV) removal increases at low pH values, and decreases as pH increases until pH 7. Sorption was found to fit the Langmuir equation and sorption capacity for the wet sorbent was higher than that for the dry one. Both sorbents showed an increased selenium sorption by rising the temperature. Redox processes between Se(IV) and the carbon sorbent are involved. Analysis by scanning electron microscope and X-ray powder diffraction for the sorbent after the reaction with acidified Se(IV) confirmed the availability of elemental selenium as particles on the sorbent surface as a result of Se(IV) reduction. Physicochemical tests showed an increase in sorbent acidity, cation exchange capacity (CEC) and surface functionality after the reaction with acidified Se(IV), indicating the oxidation processes occurring on the sorbent surface. Due to its reduction properties, the sorbent seems efficient for Se(IV) removal from aqueous solution.

Sorption of Cd(II) and Se(IV) from aqueous solution using modified rice husk was studied by Shafey [2007]. A carbonaceous sorbent was prepared from rice husk via sulfuric acid treatment. Removal of Cd(II) and Se(IV) from aqueous solution was studied varying time, pH, metal concentration, temperature and sorbent status (wet and dry). Cd(II) sorption was found fast reaching equilibrium within ~2 h while Se(IV) sorption was slow reaching equilibrium within ~200 h with better performance for the wet sorbent than for the dry. Kinetics data for both metals were found to follow pseudo-second order model. Cd(II) sorption was low at low pH values and increased with pH increase, however, Se(IV) sorption was high at low pH values, and decreased with the rise in initial pH until pH 7. A fall in the final pH was noticed with Cd(II) sorption due to the release of protons indicating an ion exchange mechanism. However, for Se(IV) sorption, a rise in the final pH was observed due to protons consumption in the process. For both metals, sorption fit well the Langmuir equation with higher uptake by rising the temperature.

Analysis by scanning electron microscope and X-ray powder diffraction for the sorbent after the reaction with acidified Se(IV) confirmed the availability of elemental selenium, Se(0), as particles on the sorbent surface. The reduction process of acidified Se(IV) to Se(0) is accompanied by surface oxidation. Physicochemical tests showed an increase in sorbent acidity, cation exchange capacity and surface functionality after the reaction with acidified Se(IV) indicating that oxidation processes took place on the sorbent surface. On the other hand, no changes in physicochemical tests were found after Cd(II) sorption indicating the absence of redox processes between Cd(II) and the sorbent.

Miquel et al.[2007] studied the sorption of Se(IV) and Se(VI) onto natural iron oxides: Goethite and hematite. In this work they studied the interaction of Se(IV), and Se(VI) with natural iron oxides hematite and goethite through two series of batch experiments at room temperature. In the first series, sorption as a function of initial selenium concentration is studied and the results have been fitted with Langmuir isotherms. In a second series of experiments, sorption is studied as a function of pH, being the main trend an increase of the sorption at acidic pH. The variation of the sorption with pH has been modeled with a triple layer surface complexation model and using the FITEQL program. The experimental data have been modelled considering for the Se(IV) the formation of the FeOSe(O)O− complex onto the hematite surface, and a

mixture of FeOSe(O)O−, and FeOSe(O)OH onto the goethite surface. For Se(VI) the surface complex considered is $FeOH_2^+$–SeO_4^{2-} on both goethite and hematite.

Literature on removal of selenium from water and waste waters is summarized in Table 2.2.1

2.3 ADSORPTION STUDIES USING BAGASSE FLY ASH, RICE HUSK ASH, GRANULAR AND POWDERED ACTIVATED CARBONS

Adsorption process has been applied for separating and purifying mixtures of a large number of substances. Adsorption has shown wide range application in the field of chemical and activated carbons (ACs) have for long, been used as important adsorbent for the removal of various adsorbates from aqueous solutions. Activated carbon has many attractive properties such as high surface area (300 - 1500 m^2/g), and high adsorption capacity for large number of adsorbates, organic chemicals, heavy metals, etc. In most instances physical adsorption has been found to prevail. Since AC can be manufactured from a variety of base materials (coal-bituminous to lignite, peat, wood, coconut shells, paper mill waste, molasses, petroleum coke, etc.) and different treatments, it has varying porous structure, physico-chemical and mechanical properties.

Table 2.3.1 presents a summary of the recent adsorption studies using BFA, RHA GAC and PAC, in batch and/or column adsorbers for the removal of various adsorbates.

Table2.2.1. Studies on removal of Selenium by various adsorbents

Adsorbents	Adsorbates	Operating conditions	Conclusions	References
Sulphuric acid-treated peanut shell	Se(IV)	Batch	Se(IV) removal rate was found slower for the dry sorbent than for the wet sorbent with removal data fitting well a pseudo-first-order model. Sorption of Se(IV) follows the Langmuir equation with an increase in uptake as temperature rises due to an expected increase in the swelling of the sorbent allowing more active sites to become available for metal ions.	Shafey [2007a]
Iron oxides	Se(IV), Se(VI)	Batch	The sorption follows a pseudo-second order kinetics.Variation of the sorption onto goethite with the selenium concentration in solution has been modelled considering a Langmuir isotherm. The main trend of the variation of the selenium sorption with pH is an increase at acidic pH.	Miquel et al. [2007]
Modified rice husk	Cd(II), Se(IV)	Batch	Kinetics data for both metals were found to follow pseudo-second order model. Cd(II) sorption was low at low pH values and increased with pH increase, however, Se(IV) sorption was high at low pH values, and decreased with the rise in initial pH until pH 7.	Shafey [2007b]
Hydrous aluminum oxide (HAO) and corundum (α-Al2O3)	Se(IV), Se(VI)	Batch	The results t highlight the fact that adsorption mechanisms of oxyanions on mineral surfaces are strongly influenced by sorbent surface properties. The results are also generally consistent with a structure-based reactivity for metal oxides.	Derek [2006]

Table2.2.1(Contd.)

Cs-covered Si(100) 2 x 1 surfaces	Se(IV), Se(VI)	Batch	Adsorption of Se on Cs/Si(100) surface system results in Se being initially adsorbed on sites different than that occupied by Cs up to 0.5 ml of Se deposition and forms SiSe compound. Higher Se deposition leads to a strong Cs–Se and Si–Cs–Se interaction, which leads to a disorder of the surface. The CsSe and Si–Se–Cs compounds are removed from the surface at about 1050 K.	Sotiropoulos et al. [2003]
Mg–Al and Zn–Al layered double hydroxides	Se(IV), Se(VI)	Batch	Experiments examining the removal of SeO32- and SeO42-from aqueous solutions by LDHs indicated that the SeO32- and SeO42- could be adsorbed on Mg–Al and Zn–Al LDHs. Adsorption isotherms could be fitted according to the Langmuir equation.	Youwen et al.[2001].
Ferrihydrite	Se(VI)	Batch	Se(VI) is removed from the water at pH below 4	USEPA (EPA/600/R-01/077)
GaAs(111)A–(2x2)surface	Se(IV), Se(VI)	Batch	The Se-induced $(2\sqrt{3} \times 2\sqrt{3})$ –R300 reconstruction is formed in the very narrow ranges of temperature and Se coverage. For the GaAs (111) A–$(2\sqrt{3} \times 2\sqrt{3})$ –R300 Se surface structure model consisting of two Se trimer and three Ga vacancies per unit cell are proposed. and have determined the atomic coordinates: the trimer has a Se–Se bond length of 2.68 A and is adsorbed at the H site of the GaAs (111)A 3 surface.	Akihiro et al. [2000]

Table 2.2.2 (Contd.)

Acidic and alkaline soils	Se(IV), Se(VI)	Batch	Adsorptionrdesorption behavior of Se was investigated in laboratory studies for surface soil samples varying in physico-chemical characteristics and mineralogical composition. In general, greater amount of Se was sorbed by acidic soils than alkaline soils; the only exception was the alkaline seleniferous soil from Barwa in northwestern India. Adsorption data for Se fitted well to Freundlich isotherm	Dhillon. [1999]
Aluminum-Oxide-Coated sand (AOCS)	Se(IV), Se(VI)	Batch	The results reveal that the adsorption rate of Se(IV) increases more rapidly than that of Se(VI) in the initial period and both of them reach meta stable equilibrium with in 60 mins. The adsorption of Se(IV) onto AOCS surface is higher than that for Se(VI) under the same system pH (3-12)	Wen-hui kuan et.al. [1997]
Iron oxyhydroxide and manganese dioxide	Se(IV), Se(VI)	Batch	The results show that the amorphous iron oxyhydroxide adsorbs more selenate and selenite than manganese dioxide at a given pH and site concentration. Selenite adsorbs more strongly than selenate on both oxides and selenate does not adsorb on manganese dioxide. Selenium adsorption decreases with increasing pH and decreasing particle concentration.	Laurie et al.[Jan1990]

Table 2.3.1. Studies on removal of various adsorbates by BFA, RHA, PAC and GAC

Adsorbents	Adsorbates	Operating conditions	Conclusions	References
Pyridine (Py)	RHA, GAC	Batch	The overall adsorption of Py on RHA and GAC is found to be in the order of GAC> RHA	Lataye et al [2008]
Methyl parathion pesticide	BFA, rice, bran, rice husk	Batch	Low cost agricultural waste namely rice bran, bagasse fly ash, M. oleifera pods, and rice husk can be effectively used to remove methyl parathion pesticide from water	Akhtar et al. [2007]
Phenol	BFA	Batch adsorption	BFA showed excellent adsorptive characteristics for the removal of phenol from wastewater samples and could be used as a very good adsorbent due to its high carbon content and the presence of silica and alumina	Srivastava et al. [2006a]
Auramine-O	BFA	Batch	The cost and adsorption characteristics favour BFA to be used as an effective adsorbent for the removal of AO dye from aqueous solution	Mall et al. [2007]
Malachite green dye	BFA	Batch adsorption	The cost and adsorption characteristics favour BFA to be used as an effective adsorbent for the removal of MG from wastewaters.	Mall et al. [2005]
2-methyl iso borneol (MIB),	PAC	Batch	Five PACs with similar surface acidity and a range of pore volumes indicated that a range of pore sizes (i.e., between 12 and 100Å) are beneficial for MIB uptake.	Tennant et al. [2007]
Surfactant sodium dodecylbenzen esulphonate	PAC	Batch	PAC enhances the transformation of ozone in aqueous phase into radicals to a greater degree.	Rivera-Utrilla et al. [2006]

Table 2.3.1 (Contd.)

Dark coloured compounds from peach pulp	PAC	Batch	The adsorption rate increased with the increasing in PAC dosage and temperature.	Arslanoglu et al. [2005]
Phenol and p-methylphenol	PAC	Sequencing batch reactor (SBR)	The reduction of the concentration of phenolic compounds in the aqueous phase through adsorption by PAC had led to enhanced bioactivity as evidenced by a reduction of lag phase in the oxygen uptake curves.	Lee and Lim [2005]
Heavy metals (Pb^{2+}, Ni^{2+})	GAC	Sequencing Batch Reactor	The SBR system with short SRT operation was found to be suitable to treat the wastewater containing heavy metals especially Pb2+ and Ni2+, because, it could remove both organic matter and heavy metals form the wastewater with high efficiency.	Sirianuntapiboon and Ungkaprasatcha [2007]
Trinitrotoluene	GAC	Fixed-bed adsorption	The adsorption capacity increased with increasing temperature and decreasing pH	Lee et al. [2007]
Ethyl-2,4-decadienoate	GAC	Fixed-bed columns	A mathematical model accounting for effective intraparticle diffusion was used to fit the kinetic adsorption data.	Diban et al. [2007]
TiO_2	GAC	Fixed bed adsorption	The GAC photo-catalysis hybrid system leads to a significantly better performance than if GAC adsorption or continuous photo-catalysis was used alone. GAC photo-catalysis hybrid system has a high removal rate of over 90% for different withdrawal rates where TiO2 and PAC were used as the catalyst.	Areerachakul et al. [2007]

Chapter – III

EXPERIMENTAL PROGRAMME

This chapter deals with the materials and methods of analysis, and the experimental procedures adopted to collect the experimental data.

3.1 MATERIALS

3.1.1 Adsorbents

Adsorption of Se(IV) was studied using four adsorbents, namely, bagasse fly ash (BFA), rice husk ash (RHA), granular activated carbon (GAC) and powdered activated carbon (PAC). BFA was obtained from a nearby sugar mill (Deoband sugar mill, U.P., India), RHA was obtained from Bhawani Paper Mills, Raebareli, U.P. (India) whereas activated carbons granules and powder were obtained from HiMedia Research Laboratory, Mumbai and S. D. Fine Chemicals, Mumbai., respectively. All adsorbents were washed with 0.1M $FeCl_3$ solution for effective removal of Se(IV). After washing, they were dried in an oven at 105 °C for 72 h. This time was sufficient to drive off the moisture. After drying, adsorbents were stored in sealed glass bottles until use.

3.1.2 Adsorbates

All the chemicals used in the study were of laboratory grade reagent (LR) grade, Sodium selenite (Na_2SeO_3) has been taken as source of Se(IV) and this was supplied by HiMedia Research Laboratory, Mumbai. The required quantity of the adsorbate was accurately weighed and dissolved in a small amount of distilled water and subsequently made up to 1 litre in a measuring flask by adding distilled water.

3.13 Other Chemicals

All other chemicals used in the study viz., acids, alkalies, $FeCl_3$, KBr, etc were supplied by S.D. Fine Chemicals, Mumbai, India.

3.2 ADSORBENT CHARACTERISATION

The characteristics of the four adsorbents were determined by using standard procedure as discussed below.

3.2.1 Proximate Analysis

Proximate analyses of the adsorbents were carried out using the procedure given in IS 1350:1984.

A small amount of the adsorbent was finely ground and a representative sample was then taken for analysis. Sample was divided into two portions. The first portion of the sample was placed in a silica crucible and its moisture was determined. To determine the moisture content, sample was weighed and kept in oven at 105 ^{0}C, for 1 h. After 1 h the dry weight of sample was taken and % moisture was determined from the difference of initial weight and final weight (dry weight). After that, the sample was heated to 750 ^{0}C in a muffle furnace and maintained at this temperature for 2 h or more till a constant weight of the residue was obtained. The weight of the residue represented the ash content of the adsorbent. The second portion of the sample was placed in a crucible, covered with a lid and heated in the furnace at 600 ^{0}C for six minutes and thereafter at 950 ^{0}C in the furnace for another six minutes. Thereafter the crucible was kept in a dessicator for cooling and then the crucible was weighed. The difference in weights was due to the loss of volatilities and moisture in the sample. The volatile matter was found by subtracting the corresponding moisture determined previously.

3.2.2 Particle Size

Particle size analyses of the adsorbents were carried out as per IS 2720 (part-4): 1985 using standard sieves.

3.2.3 Scanning Electron Microscopic (SEM) Analysis

To understand the morphology of the adsorbents before and after the adsorption of Se(IV), the SEM micrographs were taken using LEO, Model 435 VP, UK. The particles were first gold coated using Sputter Coater, Edwards S150, to provide conductivity to the samples. The SEM micrographs were taken thereafter.

3.2.4 Energy dispersive X-ray (EDAX) Analysis

Energy dispersive X-ray (EDAX) analysis of the adsorbents before and after adsorption was performed at Instiute Instrumentation Centre, IIT Roorkee to estimate the composition of various elements present in the adsorbents.

3.2.5 Fourier Transform Infra Red (FTIR) Spectral Analysis

FTIR spectrometer (Thermo Nicolet, NEXUS, USA) at dept. of chemistry, IIT-Roorkee was employed to determine the presence of functional groups in the adsorbents before and after the adsorption of Se(IV) at room temperature. Pellet (pressed-disk) technique has been used for this purpose. The spectral range was from 4000 to 400 cm^{-1}. The study was used to determine the functional groups participating in the adsorption.

3.3 BATCH EXPERIMENTAL PROGRAMME

A water-bath temperature controlled shaker (Remi Instruments, Mumbai) was used for the batch adsorption study. The temperature range for the studies was from 293 K to 323 K for Se(IV) removall. All the batch studies were performed at the constant shaking speed. For each experimental run, 50 ml aqueous solution of the known concentration of Se(IV) was taken in a 150 ml conical flask containing a known mass of the adsorbent. These flasks were agitated at a constant shaking rate of 150 rpm in a temperature controlled orbital shaker maintained at a constant temperature.

3.3.1 Effect of Initial pH (pH_0)

The sorption of Se(IV) by all adsorbents was studied over a pH_0 range of 2-10 at 303 K and over a contact time of 3 h. C_o used was 100 μg/l for Se(IV). The optimum adsorbent dosage were used in the study

3.3.2 Batch Kinetic Study

To determine the time necessary for adsorption, 50 ml of the aqueous solution containing 100 μg/l of the specific Se(IV) was taken in a series of conical flasks. Preweighed amounts of the adsorbents were added to different flasks. The flasks were kept in shaker and the aqueous solution-adsorbent mixtures were stirred at constant speed. At the end of the predetermined time, t, the flasks were withdrawn, their contents were centrifuged, and the supernatant analyzed for adsorbate concentration. Adsorption kinetics was followed for 3h and it was observed that after 1 h, there was gradual but very slow removal of the adsorbate from the solution. In order to investigate the kinetics of adsorption of the adsorbate on the adsorbents, various kinetic models, like pseudo-first-order, pseudo-second-order and intra-particle diffusion models have been used.

3.3.3 Effect of Temperature

The effect of temperature on the sorption characteristics was investigated by determining the adsorption isotherms at 293, 303, 313, and 323 K for Se(IV) removal at natural pH_0 and optimum adsorbent dosage.

3.3.4 Batch Isotherm Study

For adsorption isotherms, experiments were carried out at natural pH_0 of the samples by contacting a fixed amount of adsorbent with 50 ml of the adsorbate solutions having C_0 in the range of 100-500 μg/l. The mixture was centrifuged until equilibrium was attained and the adsorbate concentration in the supernatant solution and in the adsorbent was estimated.

Three two-parameter models, viz., Langmuir, Freundlich, and Temkin have been used to correlate the experimental equilibrium adsorption data.

3.3.5 Analysis of adsorbate concentration and Error Analysis

The concentration of Se(IV) in the aqueous solution was determined by Inductively Coupled Plasma Mass Spectroscopy (ICP-MS) at Institute Instrumentation Centre, IIT-Roorke

The percentage removal of adsorbate and equilibrium adsorption uptake in solid phase, q_e (μg/g), were calculated using the following relationships:

$$\text{Percentage adsorbate removal} = 100(C_0 - C_t)/C_0 \qquad (3.3.1)$$

$$\text{Amount of adsorbed adsorbate per g of solid, } q_t = (C_0 - C_t)V/w \qquad (3.3.2)$$

where, C_o is the initial adsorbate concentration (μg/l), C_t is the equilibrium adsorbate concentration (mg/l), V is the volume of the solution (l) and w is the mass of the adsorbent (g).

Two error functions of non-linear regression basis were employed in this study to find out the most suitable kinetic and isotherm models to represent the experimental data respectively. The hybrid fractional error function (HYBRID) and the Marquardt's percent standard deviation (MPSD) error function. These error functions are given as

$$HYBRID = \frac{100}{n-p}\sum_{i=1}^{n}\left[\frac{(q_{e,\exp} - q_{e,calc})}{q_{e,\exp}}\right]_i \qquad (3.3.3)$$

$$MPSD = 100\sqrt{\frac{1}{n-p}\sum_{i=1}^{n}\left(\frac{(q_{e,exp} - q_{e,calc})}{q_{e,exp}}\right)_i^2} \qquad (3.3.4)$$

HYBRID was developed to improve the fit of the square of errors function at low concentration values. The MPSD is similar in some respects to a geometric mean error distribution modified according to the number of degrees of freedom of the system.

3.4 THERMAL ANALYSIS OF SPENT ADSORBENTS

The spent adsorbents obtained as a result of adsorption of Se(IV) were characterized by FTIR, SEM, TGA, and DTA analyses techniques. The thermal degradation (gasification) characteristics of the blank and spent adsorbents were studied using the thermo-gravimetric and differential analysis techniques. The thermal degradation of the adsorbents was carried out non-isothermally at the Institute Instrumentation Centre, IIT, Roorkee using the TGA analyzer from Perkin Elmer, Pyris Diamond.

In the present study, the operating pressure was kept slightly positive. The samples were prepared carefully after crushing and sieving so as to obtain homogeneous material properties. The sample was uniformly spread over the crucible base in all the experiments and the quantity of sample taken was 5-10 mg in all the runs. The oxidation runs were taken at heating rate of 25 K/min under an oxidizing atmosphere (flowing moisture-free air) for gasification. The tests were conducted over a range of temperature from the ambient temperature to 1000 ^{0}C. Flow rate of nitrogen/air was maintained at 200 ml/min.

The weight loss, during thermal heating was continuously recorded and downloaded using the software, Muse, Pyris Diamond. The instrument also provided the continuous recording of the differential thermal gravimetry (DTG) and differential thermal analysis (DTA) as a function of sample temperature and time. The TG, DTG and DTA curves obtained in each case were analyzed to understand the behavior of thermal degradation.

Chapter –IV

RESULTS AND DISCUSSION

4.1 GENERAL

This chapter presents the results and discussion pertaining to adsorption of Se(IV) from water onto bagasse fly ash (BFA), rice husk ash(RHA), granular activated carbon (GAC) and powdered activated carbon (PAC). This chapter has been divided into the following sections:

1. Characterization of adsorbents
2. Batch adsorption study
3. Thermal degradation of spent adsprbents

4.2 CHARACTERIZATION OF ADSORBENTS

All adsorbents were treated with 0.1M $FeCl_3$ solution. The physico-chemical characteristics of the adsorbents such as proximate analysis carried out. The energy dispersive X-ray (EDAX) analysis, scanning electron microscopy (SEM) analyses and fourier transform infra red (FTIR) spectral analysis were used to study the structural and morphological characteristics of adsorbents.

4.2.1 Physico-chemical Characterization of Adsorbents

Proximate analysis and particle size of the four adsorbents are presented in Table 4.2.1. It is observed that the amount of ash is very high in BFA and RHA in comparison to that in PAC and GAC. High amount of ash indicates that BFA and RHA are basically inorganic in nature. The amount of carbon content is highest in PAC followed by GAC, BFA and RHA. Due to low carbon content, BFA and RHA are expected to have low porosity, and thereby low surface area.

The SEM micrographs of $FeCl_3$ coated adsorbents and Se(IV) loaded adsorbents are shown in Figs. 4.2.1 and 4.2.2. These figures reveal surface texture and porosity of the blank and loaded adsorbents. It can be inferred from these figures that the surface texture of the blank adsorbents changes drastically after the loading of the adsorbates.

Energy dispersive X-ray analysis (EDAX) analysis of the adsorbents before and after adsorption was performed to estimate the composition of various elements present in the adsorbents. EDAX spectra indicates presence of elemental selenium after adsorption onto all adsorbents as shown in Fig. 4.2.3 and 4.2.4. It indicates that at the adsorbent surface Se(IV) was reduced to elemental selenium.

Table 4.2.1. Physical characteristics of adsorbents.

Characteristics	BFA	RHA	GAC	PAC
Proximate analysis				
Moisture (%)	12.35	10.07	7.60	6.65
Volatile matter (%)	11.16	15.03	11.73	7.76
Ash (%)	57.26	69.61	8.59	5.44
Fixed Carbon (%)	20.55	5.36	72.08	80.15
Average particle size (μm)	381	412	2-5 mm	8

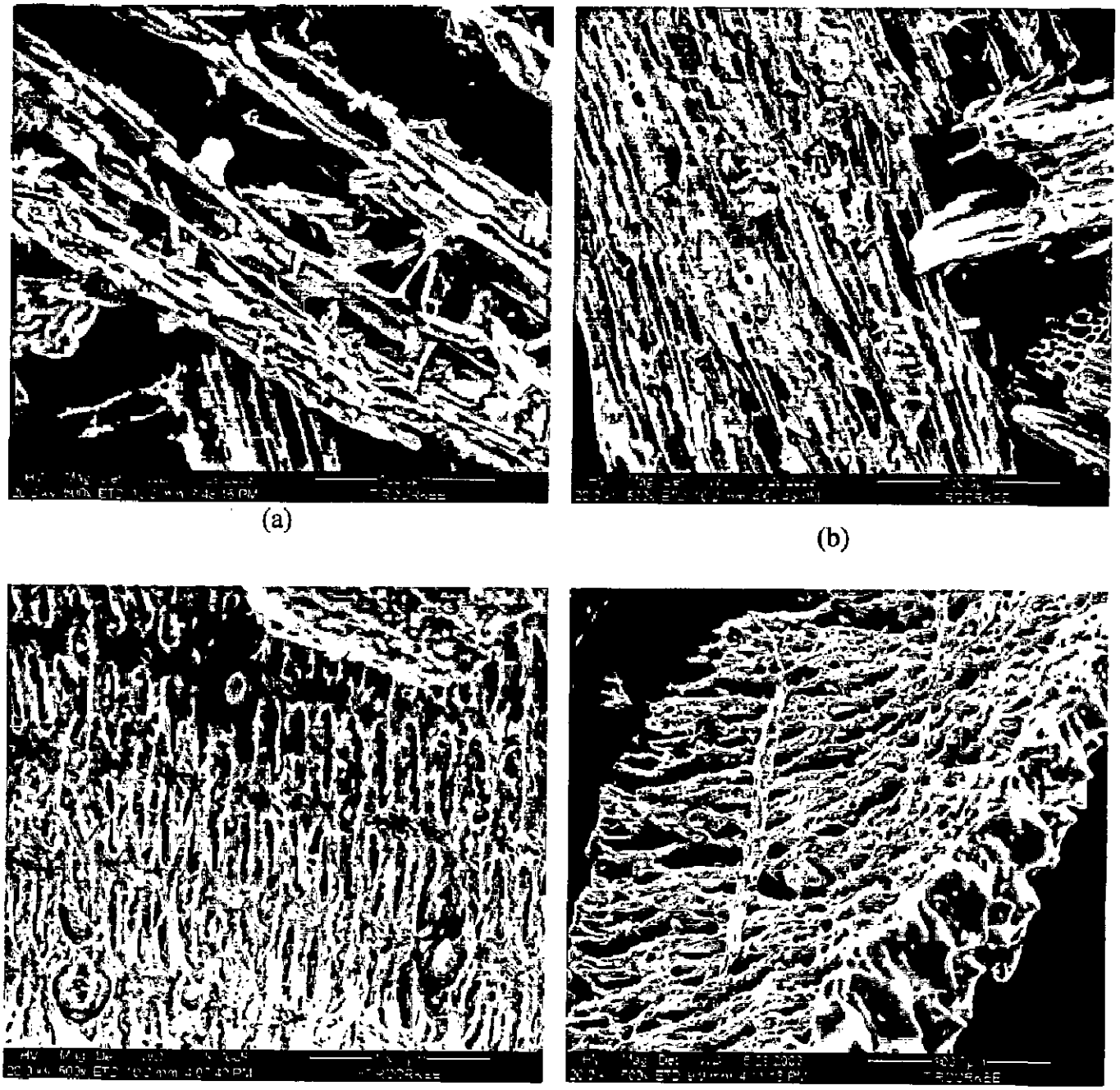

(a) (b)

(c) (d)

Fig. 4.2.1. SEM micrographs of of (a) blank ($FeCl_3$ coated) (b) Se(IV) loaded BFA, (c) blank ($FeCl_3$ coated)and (d) Se(IV) loaded RHA at 500X.

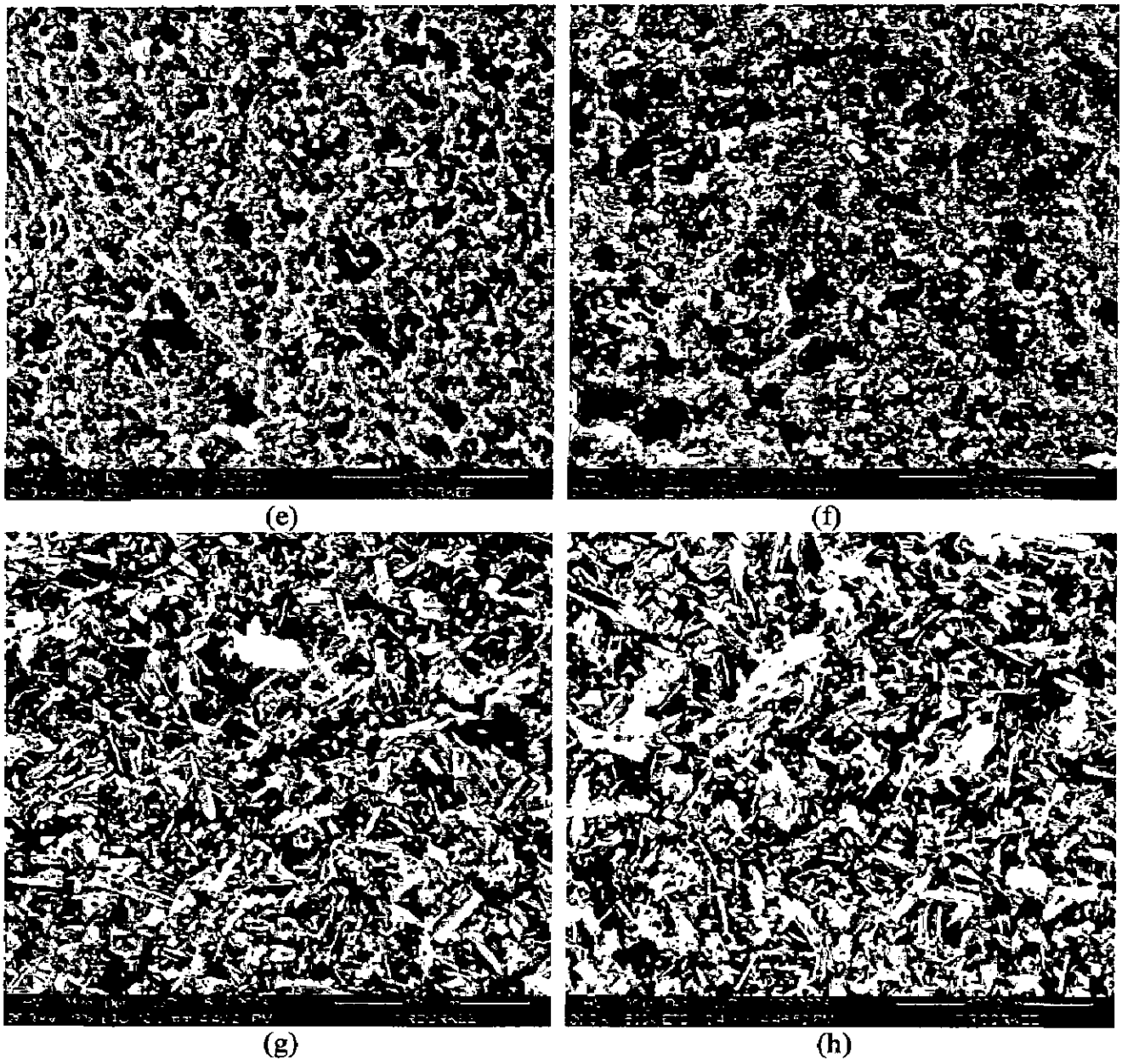

Fig. 4.2.2. SEM micrographs of of (e) blank ($FeCl_3$ coated) (f) Se(IV) loaded GAC, (g) blank ($FeCl_3$ coated) and (h) Se(IV) looaded PAC at 500X.

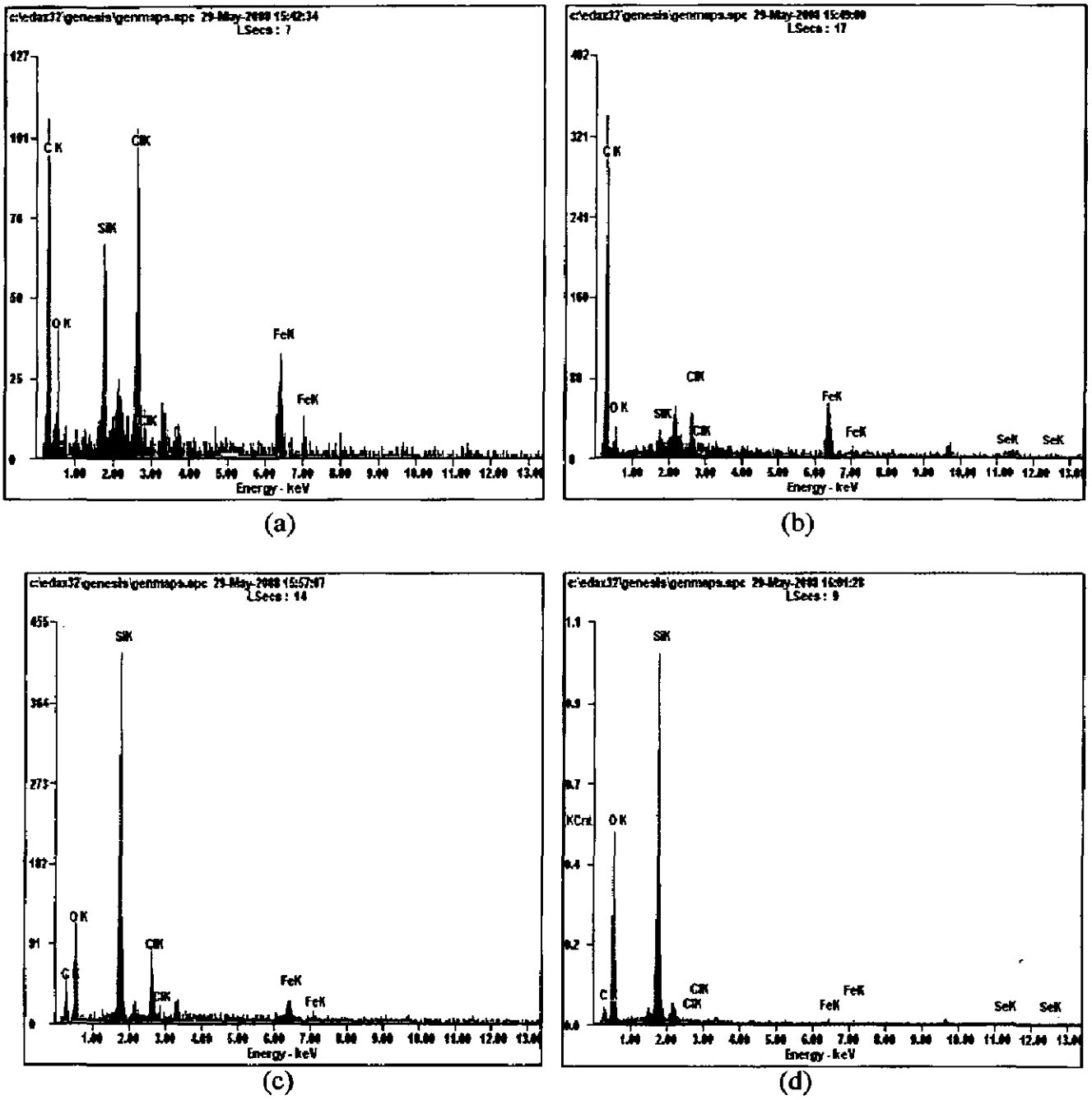

Fig. 4.2.3. EDAX analysis of (a) blank ($FeCl_3$ coated) and (b) Se(IV) loaded BFA, (c) blank ($FeCl_3$ coated) and (d) Se(IV) loaded RHA

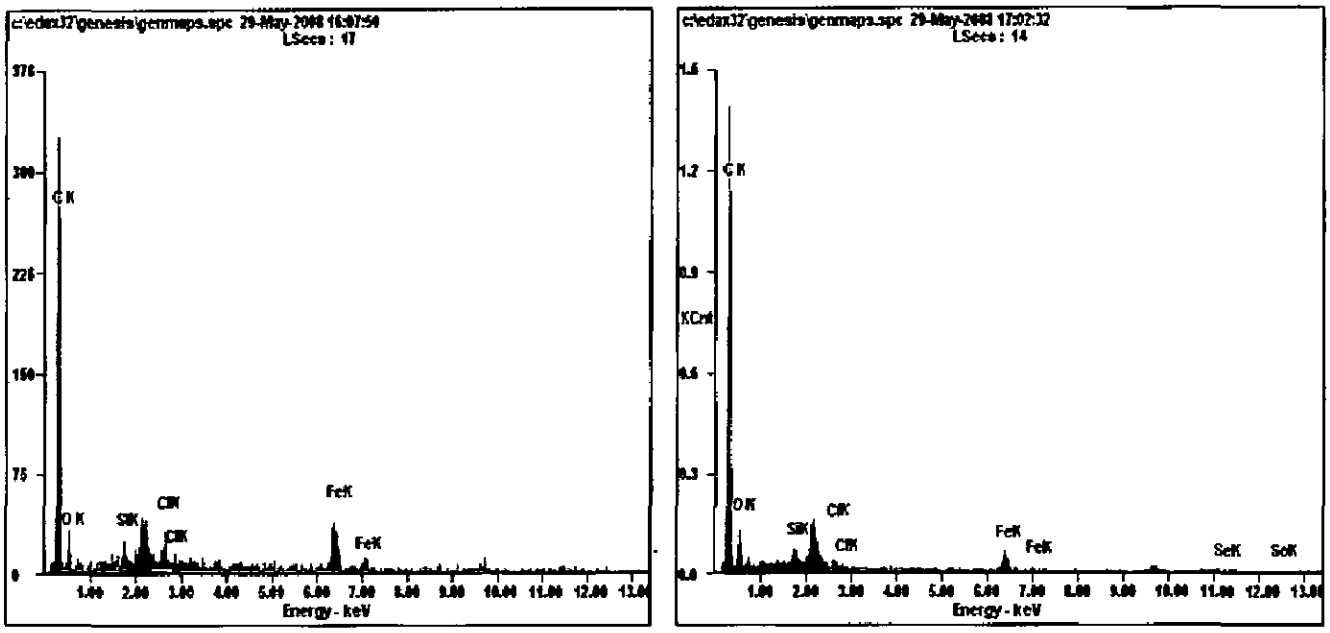

(e) (f)

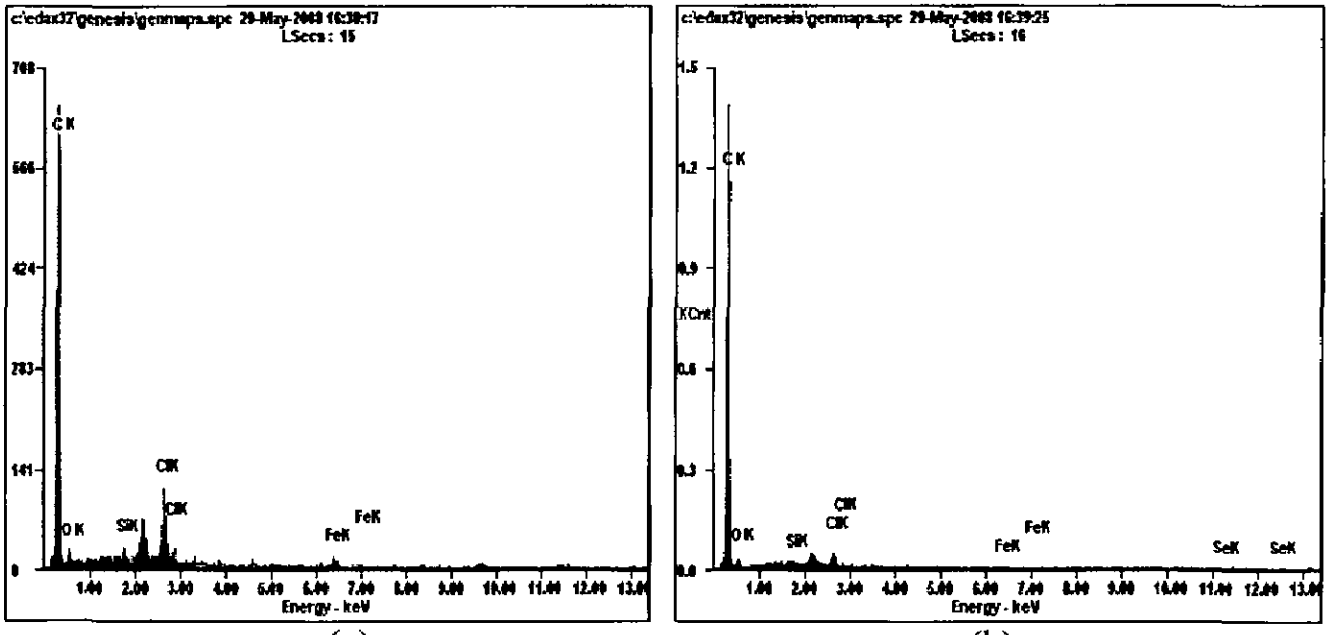

(g) (h)

Fig. 4.2.4. EDAX analysis of (e) blank ($FeCl_3$ coated) (f) Se(IV) loaded GAC, (g) blank ($FeCl_3$ coated) and (h) Se(IV) looaded PAC

4.2.2 FTIR Spectroscopy of the Adsorbents

The chemical structure of the adsorbents is of vital importance in understanding the sorption process. The adsorption capacity of adsorbents is strongly influenced by the chemical structure of their surface. The carbon-oxygen functional groups are by far the most important structures that influence the surface characteristics and surface behavior of adsorbents. The functional groups suggested most often are (I) carboxyl groups, (II) phenolic hydroxyl groups, (III) carbonyl groups (e.g. quinone-type), and (IV) lactone groups (e.g. fluorescein-type).[Kumar, 2007]. The FTIR technique is an important tool to identify the characteristic functional groups, which are instrumental in adsorption of Se(IV).

The FTIR spectra of the $FeCl_3$ coated and Se(IV)-loaded BFA, RHA, GAC and PAC are shown in Figs. 4.2.5 through 4.2.8, respectively. A broad band between 3100 and 3700 cm^{-1} in all the adsorbents is indicative of the presence of both free and hydrogen bonded OH groups on the adsorbent surface. This stretching is due to both the silanol groups (Si-OH) and adsorbed water (peak at 3400 cm^{-1}) on the surface. C-O group stretching from aldehydes and ketones can also be inferred from peaks in the region of 1600 cm^{-1}. These FTIR spectra also show transmittance around ~1100 cm^{-1} region due to the vibration of the CO group in lactones and due to Si-O-Si and –C-OH stretching and –OH deformation.

Fig. 4.2.5 shows the FTIR spectra of $FeCl_3$ coated and Se(IV)-loaded BFA; appearance of a band at 3481 cm^{-1} which is assigned to O-H hydrogen bonding while the bands at 2921 cm^{-1} and 2913 cm^{-1} are assigned to O-H stretching vibration originating in the molecule. Peaks at 1628 cm^{-1} show the medium bands of N-H (amines). With the loading of Se(IV) onto BFA, shifting of the peaks is seen from about 902 and 1021 cm^{-1}. This means that the functional groups at these wave numbers participate in the Se(IV) adsorption. The shifting occurs both to higher and lower wave numbers.

Fig 4.2.6 shows bands appearing at 3451 and 3457 cm^{-1} in spectra of RHA indicate presence of O-H bonding. C=C stretching indicates presence of bands at 1633 cm^{-1}.

In GAC spectra (Fig 4.2.7), broad bands appear at 3440 and 3436 cm^{-1} assigned to O-H hydrogen bonding. The peak at 2923 cm^{-1} shows the C-H alkanes. Peaks at 1632

cm^{-1} and 1629 cm^{-1} show the medium bands of N-H (amines). Peaks at 2619 cm^{-1} indicates C-H alkanes and peaks at 1384 cm^{-1} indicate symmetrical CO_2^- stretching. Shifting of various bands occur in spectra of Se(IV) loaded GAC. Small bands appearing at 1736 cm^{-1} and 1433 cm^{-1}, represent O-H stretching. Bands at 661 cm^{-1} and 669 cm^{-1} represent the presence of alkynes

In Fig. 4.2.8, bands appearing at 3434 cm^{-1} in spectra of PAC indicate hydrogen bonding; and at 2923 cm^{-1} is assigned to O-H stretching vibration originating in the molecule. Bands at 669 cm^{-1} represent the presence of alkynes In Se(IV) loaded spectra of PAC adsorption system,new bands highlight the spectra. Bands appearing at 1254 cm^{-1} and 1165 cm^{-1} are due to CH_2 deformation For Se(IV) loaded PAC, large numbers of peaks corresponding to various groups disappear after the Se(IV) loading which indicates utilization of these groups during sorption process

Although some inference can be drawn about the surface functional groups participating in the adsorption process from FTIR spectra, the weak and broad bands do not provide any authentic information about the nature of the surface oxides.

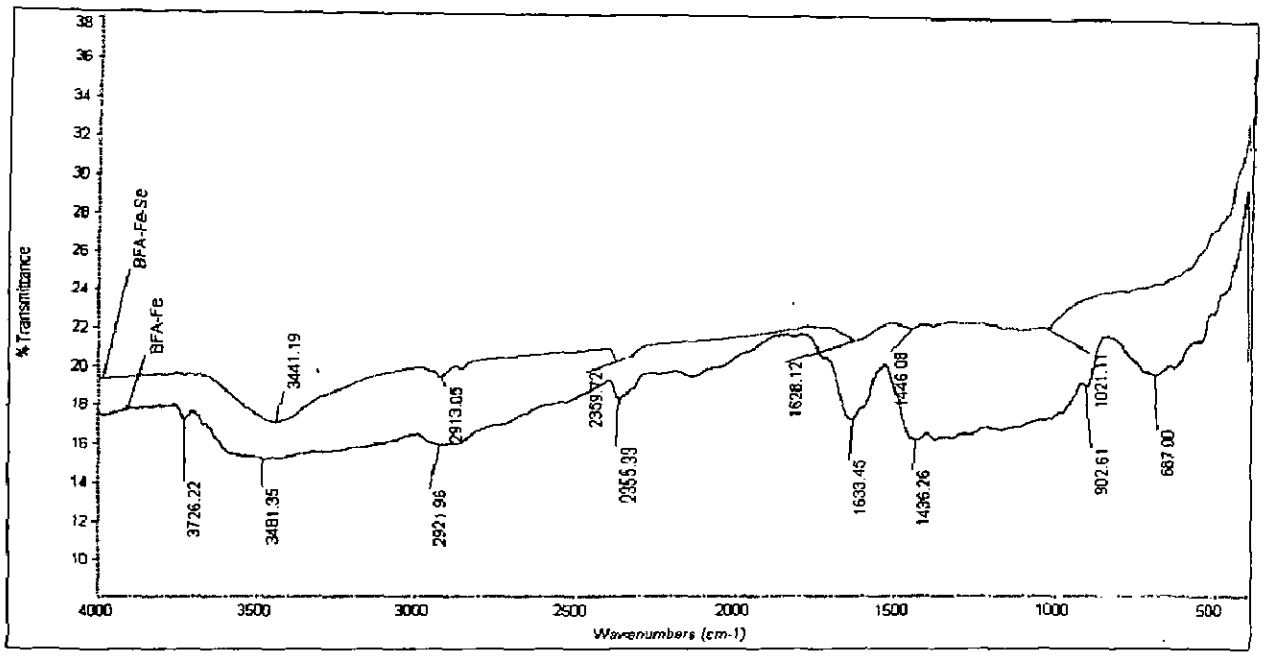

Fig. 4.2.5. FTIR spectra of BFA($FeCl_3$ coated) and Se(IV)-loaded BFA($FeCl_3$ coated)

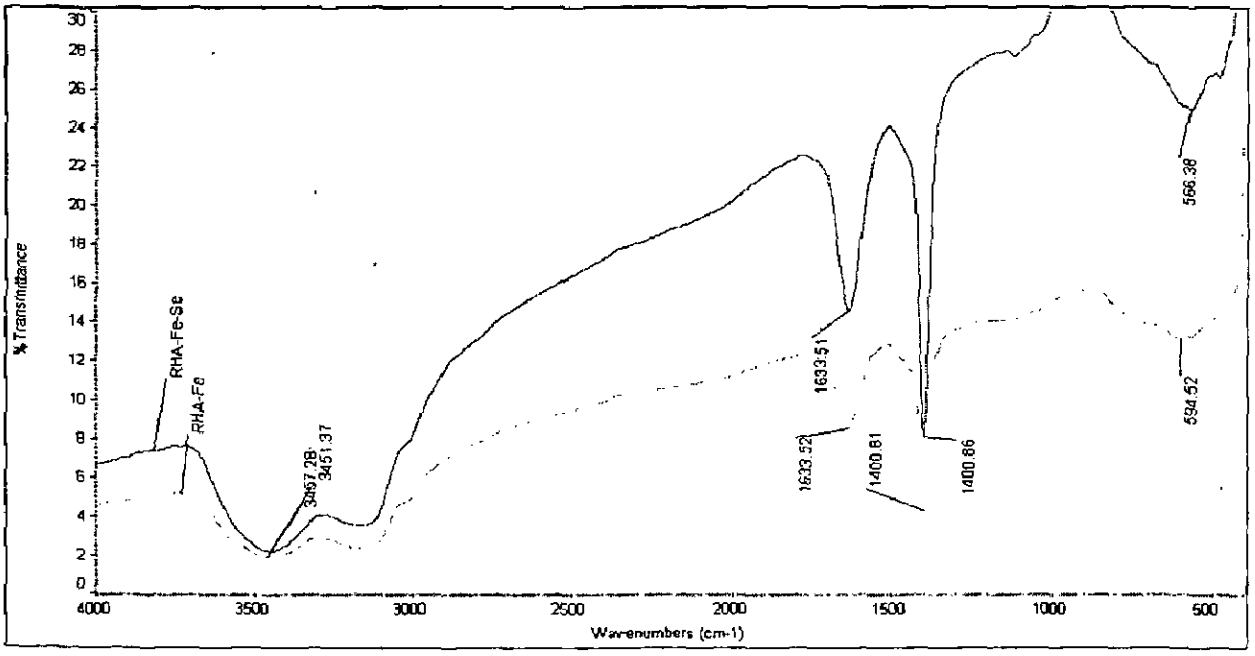

Fig. 4.2.6. FTIR spectra of RHA($FeCl_3$ coated) and Se(IV)-loaded RHA($FeCl_3$ coated)

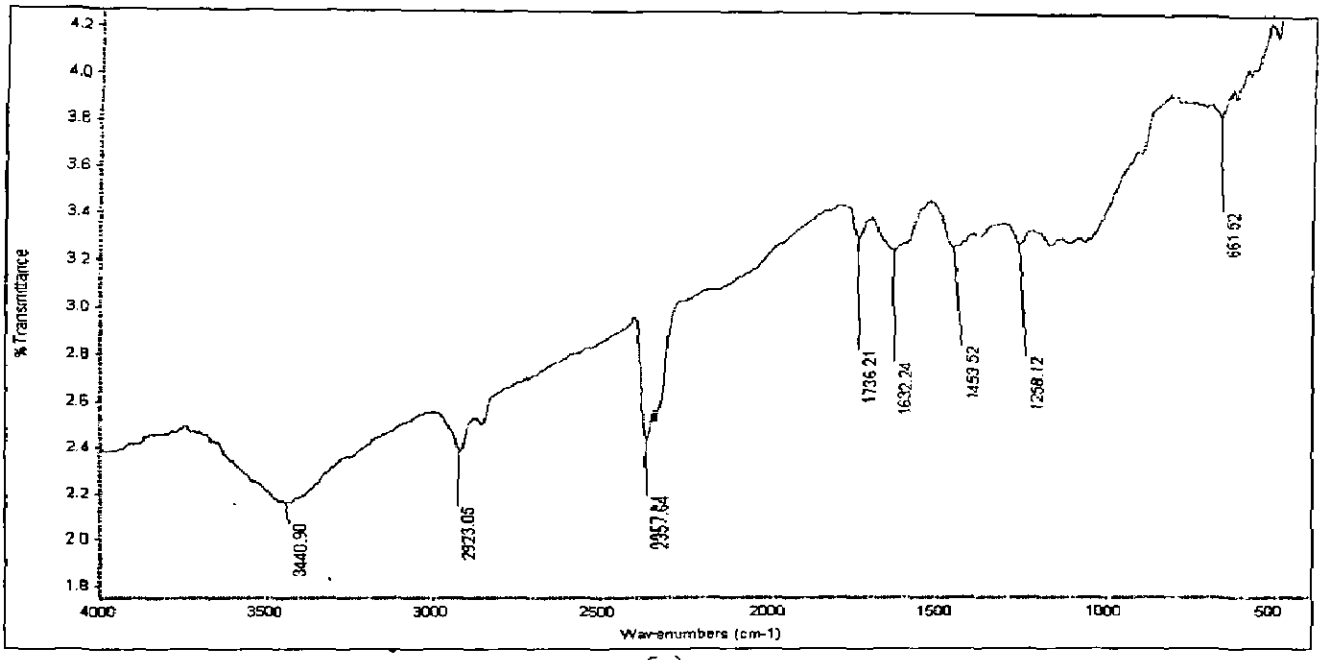

(a)

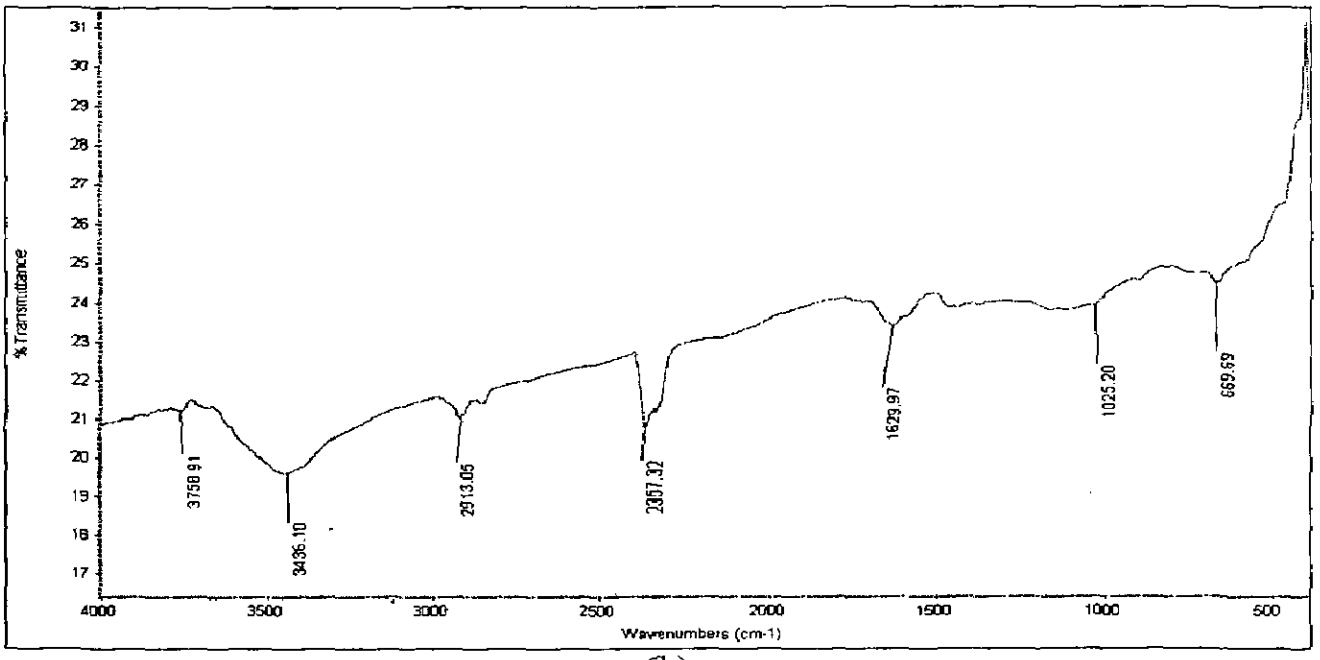

(b)

Fig. 4.2.7. FTIR spectra of (a) GAC ($FeCl_3$ coated and (b) Se(IV)-loaded GAC ($FeCl_3$ coated)

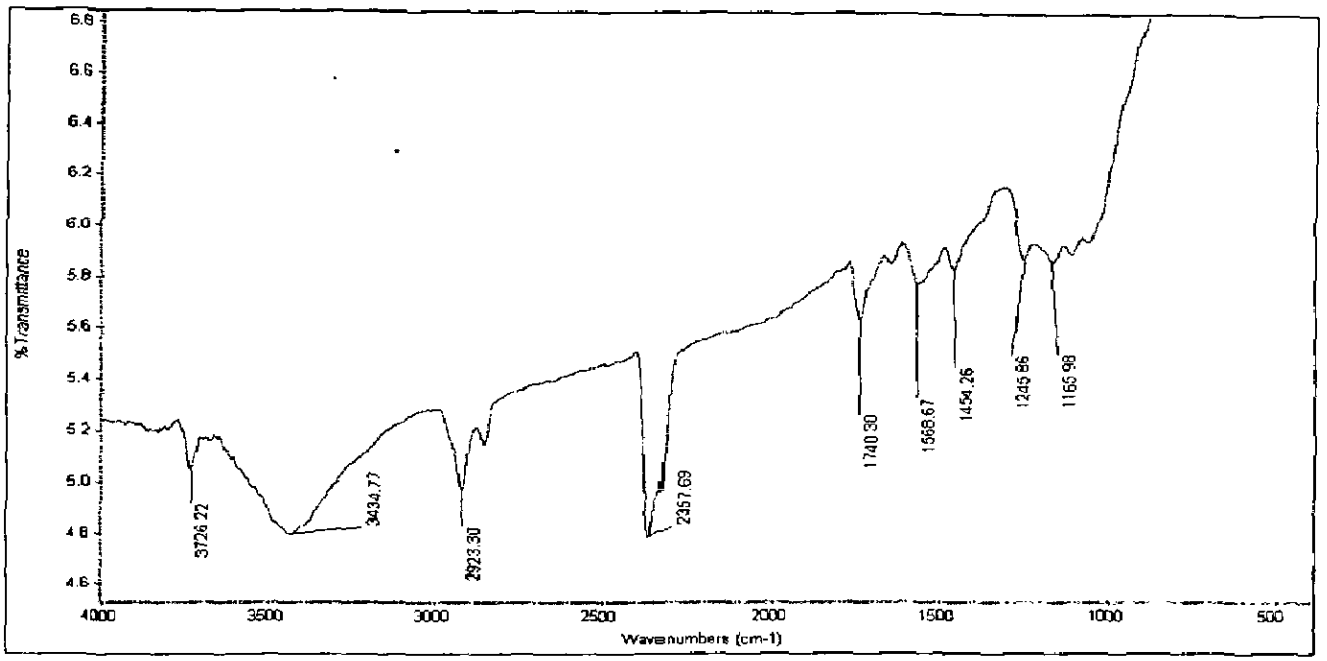

(a)

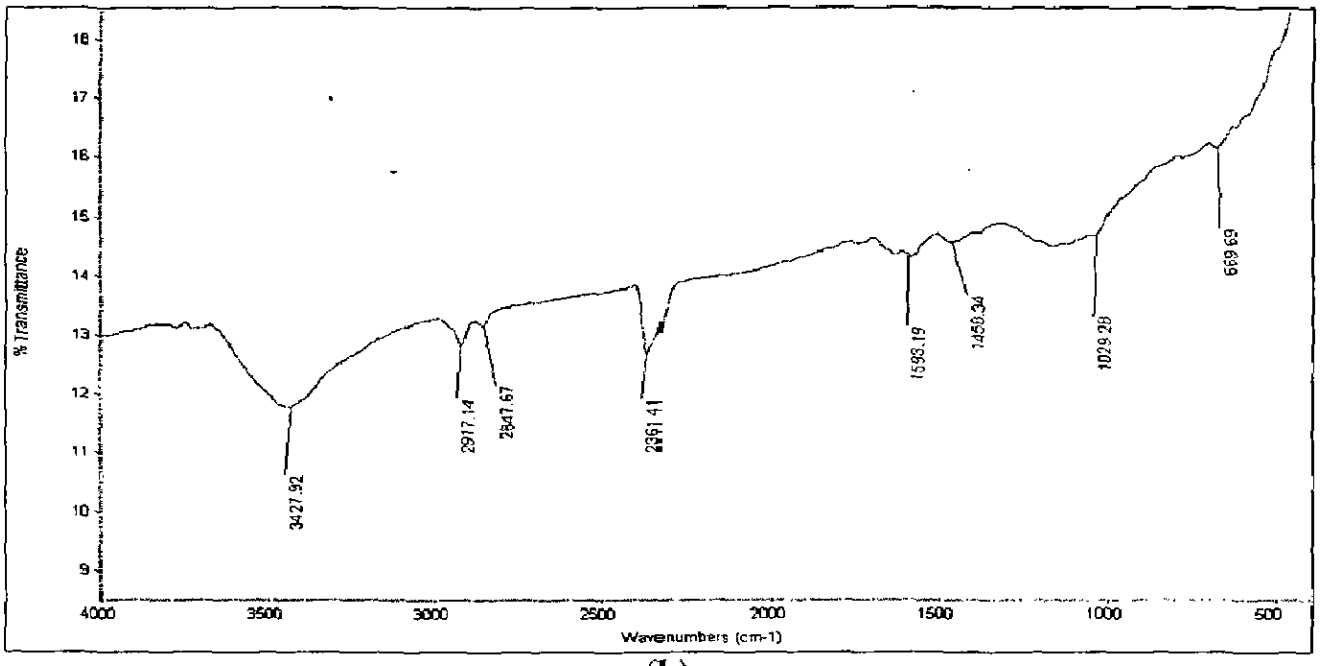

(b)

Fig. 4.2.8. FTIR spectra of (a) PAC($FeCl_3$ coated) and (b) Se(IV)-loaded PAC($FeCl_3$ coated)

4.3 BATCH ADSORPTION STUDY

Batch adsorption experiments were conducted for the removal of Selenium from water by $FeCl_3$ coated BFA, RHA, GAC and PAC. Evaluation of various parameters, viz. adsorbent dose (w), initial pH (pH_0), contact time (t),initial concentration (C_0) and temperature is of vital importance in the design of any adsorption system for the removal of Se(IV). The effect of these parameters on the adsorption of Se(IV) onto $FeCl_3$ coated BFA, RHA, GAC and PAC are presented below.

4.3.1 Effect of adsorbent dosage (w)

The effect of w on the uptake of Se(IV) onto $FeCl_3$ coated BFA, RHA, GAC and PAC was studied for C_o = 100 μg/l and is shown in Fig. 4.3.1. For Se-BFA, Se-RHA, Se-GAC and Se-PAC systems, the optimum adsorbent dosage. w was found to be 4, 6, 10 and 8 g/l, respectively. It is found that the removal of Se(IV) by any of the adsorbents increases with an increase in the adsorbent dosage initially and, thereafter, becomes constant after some value of w. This value is taken as the optimum dosage, w.

The increase in adsorption with the adsorbent dosage can be attributed to the availability of greater surface area and larger number of adsorption sites. At $w < w_{optimum}$, the adsorbent surface becomes saturated with Se(IV) and the residual Se(IV) concentration in the solution is large. With an increase in w, the Se(IV) removal increases due to increased Se(IV) uptake by the increased amount of adsorbent. For $w < w_{optimum}$, the incremental removal of Se(IV) becomes very small as the surface Se(IV) concentration and the solution Se(IV) concentration come to near equilibrium with each other. At about $w < w_{optimum}$, the removal efficiency becomes almost constant for the removal of Se(IV) onto $FeCl_3$ coated BFA, RHA, GAC and PAC.

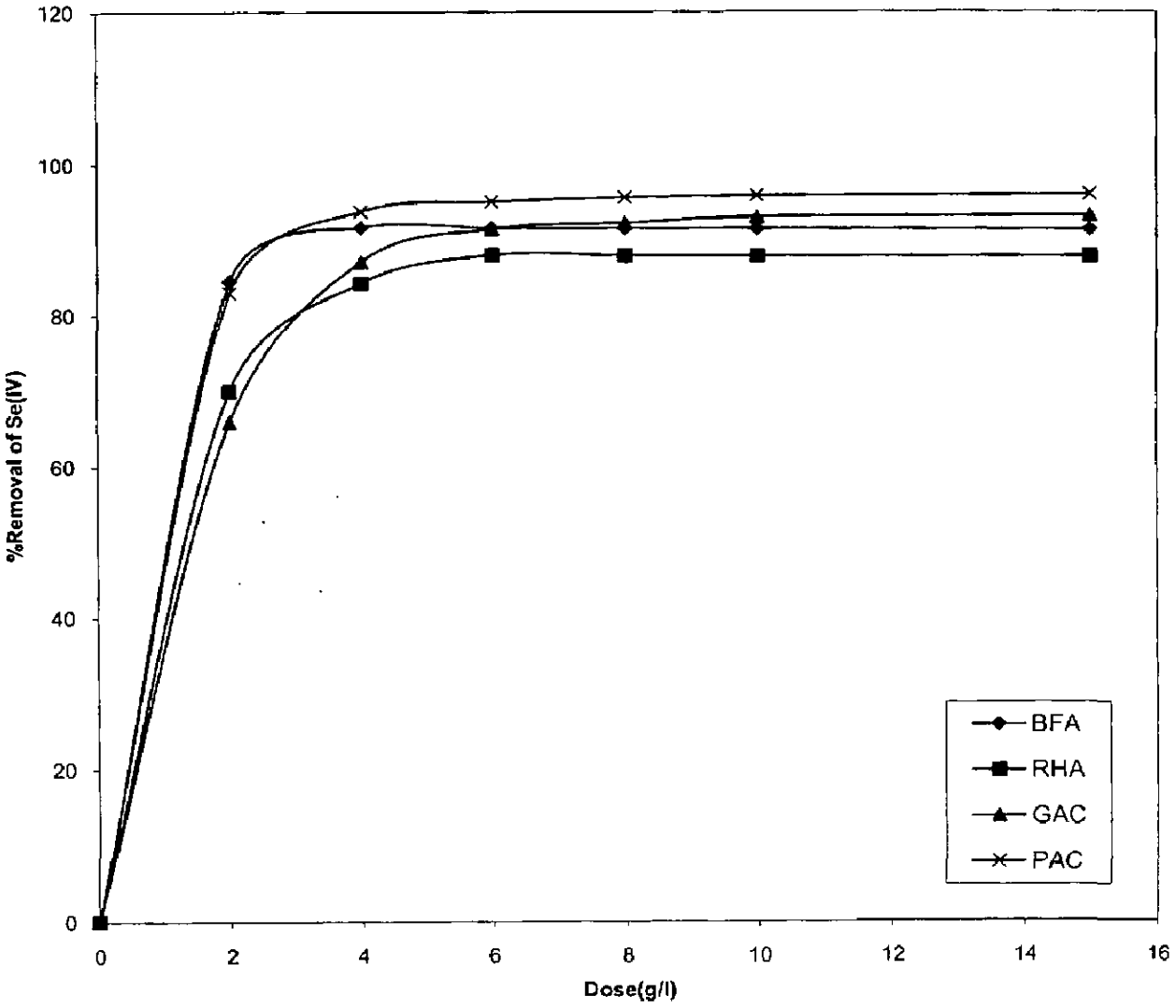

Fig. 4.3.1. Effect of adsorbent dose on the removal of Se by $FeCl_3$ coated BFA, RHA, GAC and PAC. T=303K, t=3 h, C_0=100 μg/l

4.3.2 Effect of contact time

The effect of contact time on the removal of Se(IV) onto $FeCl_3$ coated BFA,RHA, GAC and PAC shown in Fig. 4.3.2. The rate of removal of Se(IV) from water is very fast with all the adsorbents. This is obvious from the fact that a large number of vacant surface sites are available for the adsorption during the initial stage and with the passage of time, the remaining vacant surface sites are difficult to be occupied due to repulsive forces between the solute molecules on the solid phase and in the bulk liquid phase.

For Se-BFA and Se-RHA systems, the adsorption of Se(IV) remains almost constant and the difference between the adsorptive uptake at 2 h and 3 h and is less than 1% of that at 5 h. Therefore, a steady-state approximation was assumed and a quasi-equilibrium situation was considered at t = 2 h. The rate of removal of Se(IV) with GAC and PAC is found to be fast, with more than 61 % removal for GAC and more than 43 % removal for PAC obtained within 10 min. A steady-state approximation was considered at t=30 min.for GAC and t= 60 min. for PAC. All the batch experiments were therefore, conducted with a contact time of 2h for systems Se-BFA and Se-RHA: and with contact time of 30 min and 60 min for GAC and PAC respectively, under vigorous shaking conditions at natural *pH* in aqueous solutions. *pH* was not adjusted during the experiments. Based on these results kinetic studies, viz. pseudo first order, psedo second order, weber moris are perfomed on all Se(IV) adsorbent systems.

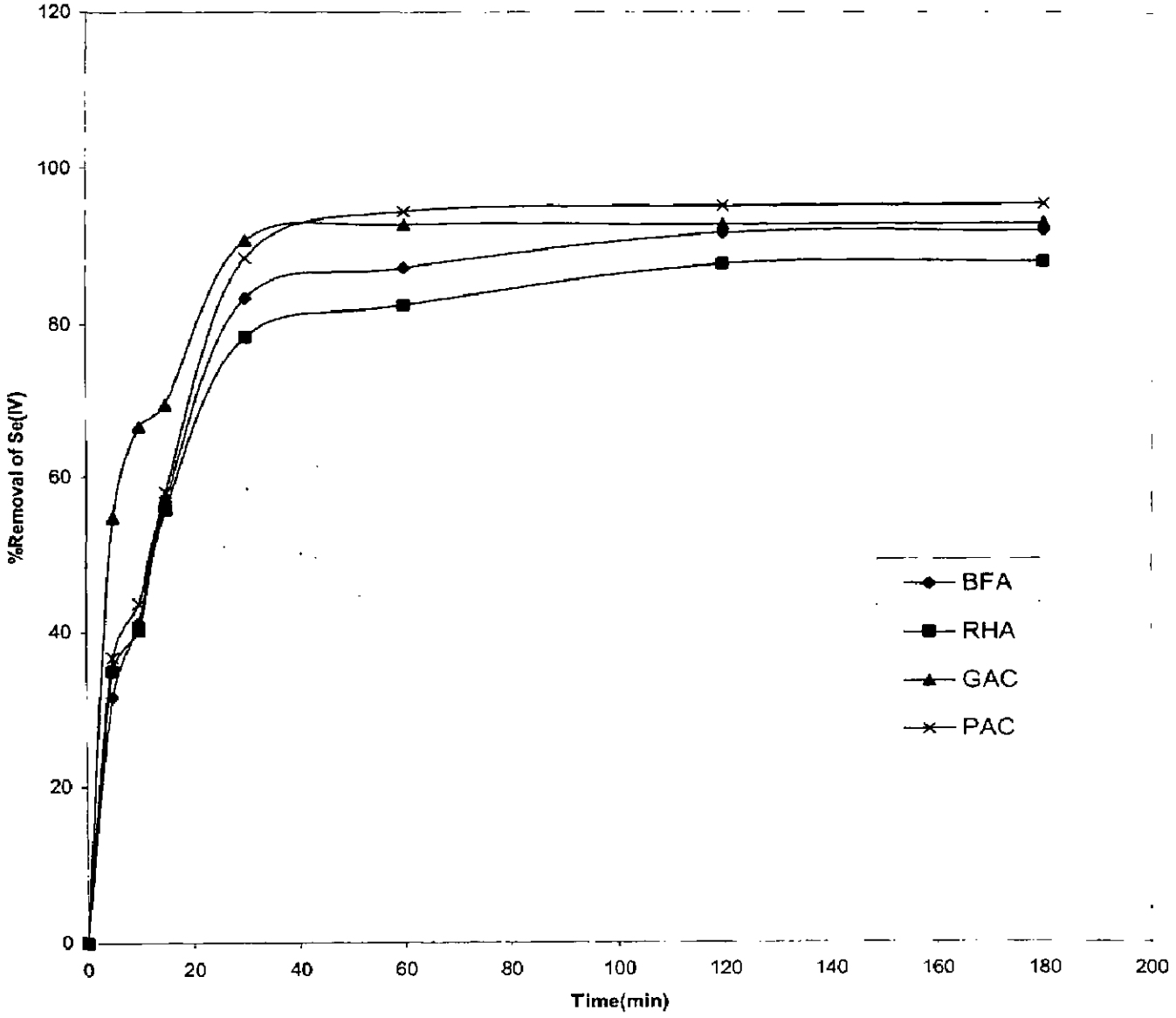

Fig. 4.3.2 Effect of contact time on % removal of Se(IV) by $FeCl_3$ coated BFA, RHA,GAC and PAC. T=303K, C_0=100 µg/l

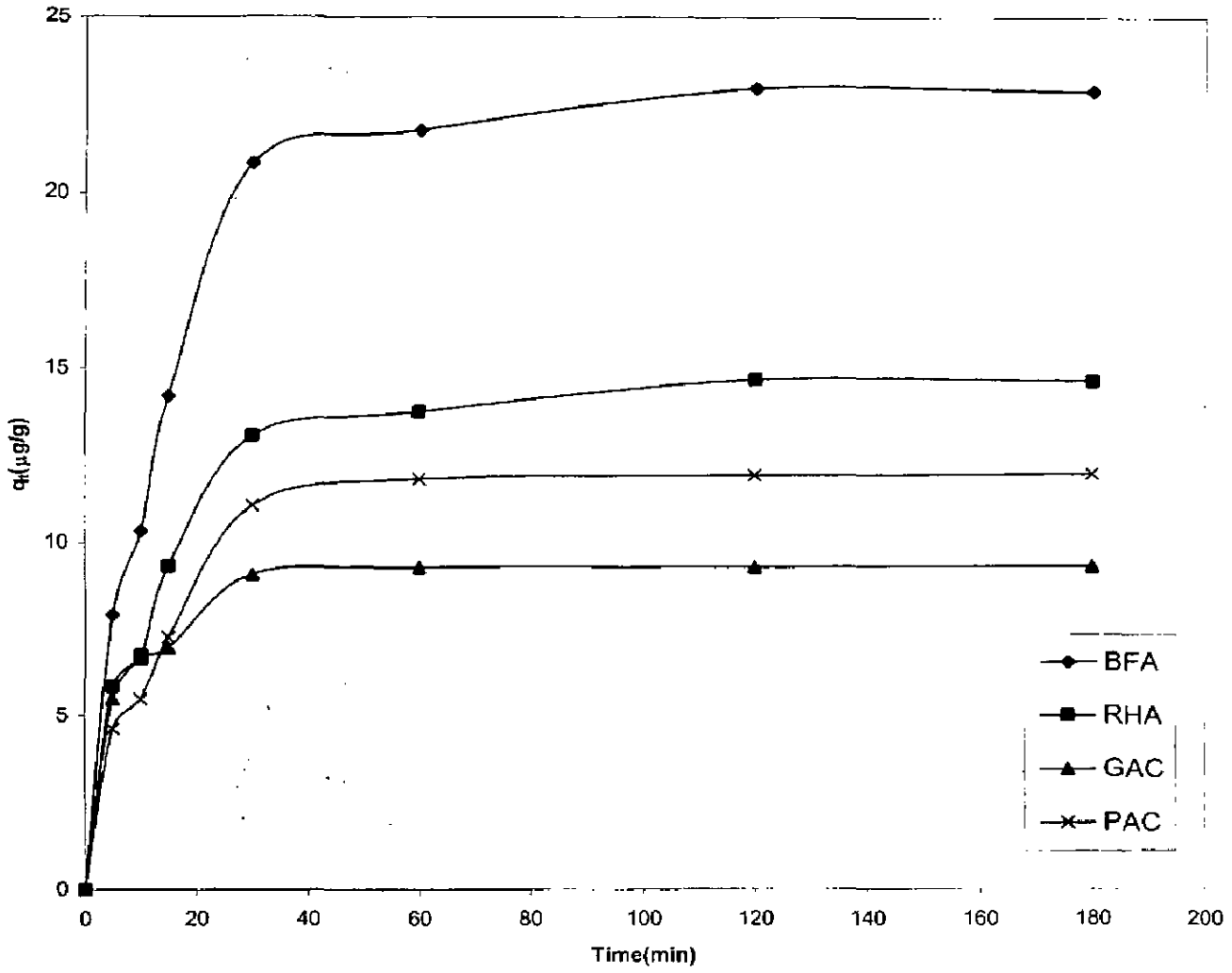

Fig. 4.3.3. Effect of contact time on the removal of Se(IV) by $FeCl_3$ coated BFA, RHA, GAC and RHA at natural *pH*. *T*=303K, C_0=100µg/l.

4.3.3 Change in *pH*

The pH_0 of the aqueous solution with C_0 = 100 µg/l of Se(IV) is found to be 6.46. With the addition of the adsorbents, the solution *pH* changes. The intial *pH* of all the adsorbent systems is varied from 2 to 10 and the % removal at equilibrium is obtained as shown in Fig. 4.3.4. With all the adsorbents, it is found that the sorption of Se(IV) of decreases at alkaline *pH* and maximum removal is obtained at *pH* 2 to 3.

Se(IV) species in aqueous solution include selenious acid (H_2SeO_3), biselenite ($HSeO_3^-$) and selenite(SeO_3^{2-}). Between *pH* 3.5 and 9.0, biselenite ion is the predominant ion in water. Above *pH* 9.0 selenite species dominates and as pH decreases below *pH* 3.5, selenious acid dominates. Se(IV) sorption decreases at alkaline pH due to the decrease of the fraction of the aqueous species of $HSeO_3^-$.

For all systems, the final *pH* changes from its initial value of 6.46 to around 2.5. The difference in the pH_f for the adsorption of the Se(IV) on different adsorbents reinforces the differences in the surface functional groups of BFA,RHA, GAC and PAC.

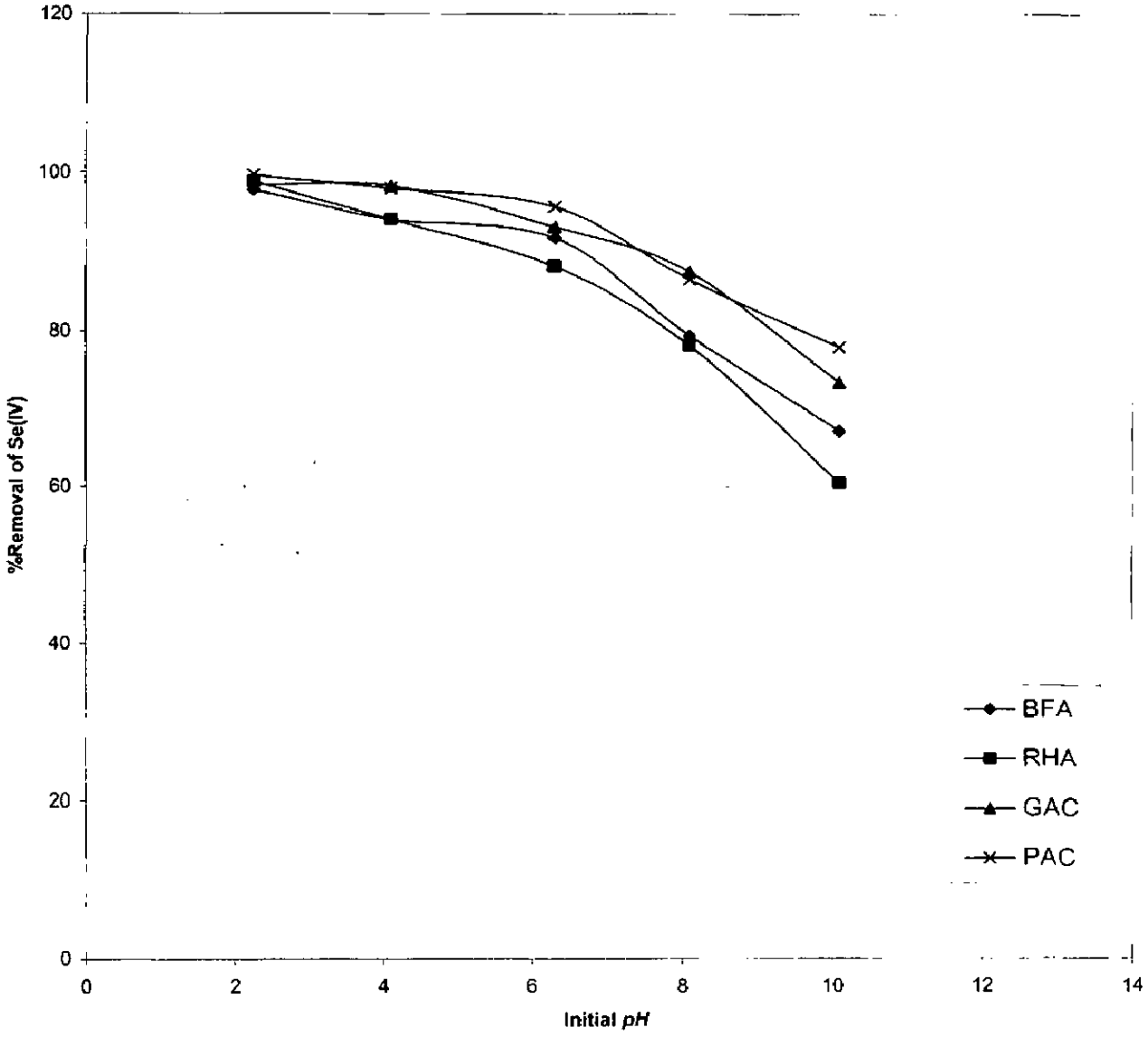

Fig. 4. 3.4 Effect of initial pH on % removal of of Se(IV) by $FeCl_3$ coated BFA, RHA,GAC and PAC . T=303K, C_0=100μg/l

4.3.4 Adsorption Kinetic Study

The frequently used kinetic models, viz. pseudo-first-order, pseudo-second-order and intraparticle diffusion models, have been tested to investigate the adsorption process of Se(IV) onto $FeCl_3$ coated BFA, RHA, GAC and PAC.

4.3.4.1 Pseudo-first-order model

The pseudo-second-order model can be represented in the following form

$$\log(q_e - q_t) = \log q_e - \frac{k_f}{2.303} t \qquad (4.3.1)$$

This equation is, however, valid only for the initial period of adsorption. Various investigators have erroneously fitted this equation to the adsorbate uptake data for later periods, ignoring the data of the initial period for the model fitting. The values of the pseudo-first-order adsorption rate constant (k_f) (Tables 4.3.1) are determined from the above Eq.4.3.1 by plotting $\log(q_e - q_t)$ against t for Se(IV) adsorption onto all the adsorbents with C_0=100 μg/l at 303 K for the first 30 min only. Experimental results did not follow first-order kinetics given by as there was difference in two important aspects: (i) $k_f(q_e - q_t)$ does not represent the number of available sites, and (ii) $\log q_e$ was not equal to the intercept of the plot of $\log(q_e - q_t)$ against t.

4.3.4.2 Pseudo-second-order model

The pseudo-second-order model can be represented in the following form

$$q_t = \frac{ht}{1 + k_s q_e t} \qquad (4.3.2)$$

where, $h = k_S q_e^2$ (4.3.3)

Eq. 4.3.2 has been fitted to the experimental data using a non-linear regression method. This has been accomplished by minimizing the respective coefficient of determination between experimental data and predicted values. The best-fit values of h, q_e and k_s along with the correlation coefficients for all the adsorbate–adsorbent systems and the optimum values of kinetic parameters are given in Table 4.3.1 for all the systems

with C_0=100 μg/l used in the present study. The plot of the experimental adsorption capacity q_t with t is shown in Fig 4.3.3.

The $q_{e,\exp}$ and the $q_{e,cal}$ values for the pseudo-first-order model and pseudo-second-order models are also shown in Tables 4.3.1. The $q_{e,exp}$ and the $q_{e,cal}$ values from the pseudo-second-order kinetic model are very close to each other. The calculated correlation coefficients are also closer to unity for pseudo-second-order kinetics than that for the pseudo first-order kinetic model. Therefore, the sorption can be approximated more appropriately by the pseudo-second-order kinetic model than the pseudo-first-order kinetic model for the adsorption of Se(IV) onto $FeCl_3$ coated BFA, RHA, GAC and PAC.

4.3.5 Intra-particle Diffusion Study

The adsorbate transport from the solution phase to the surface of the adsorbent particles occurs in several steps,. The overall adsorption process may be controlled either by one or more steps, e.g. film or external diffusion, pore diffusion, surface diffusion and adsorption on the pore surface, or a combination of more than one step. In a rapidly stirred batch adsorption, the diffusive mass transfer can be related by an apparent diffusion coefficient, which will fit the experimental sorption-rate data. The possibility of intra-particle diffusion was explored by using the intra-particle diffusion model

$$q_t = k_{id} t^{0.5} + I \qquad (4.3.4)$$

where, k_{id} is the intra-particle diffusion rate constant ($\mu g/g\,min^{0.5}$) and I ($\mu g/g$) is a constant that gives idea about the thickness of the boundary layer, i.e., larger the value of I, the greater is the boundary layer effect [Kumar, 2007]. If the Weber-Morris plot of q_t versus $t^{0.5}$ satisfies the linear relationship with the experimental data, then the sorption process is found to be controlled by intra-particle diffusion only. However, if the data exhibit multi-linear plots, then two or more steps influence the sorption process. The mathematical dependence of fractional uptake of adsorbate on $t^{0.5}$ is obtained if the sorption process is considered to be influenced by diffusion in the cylindrical (or spherical) and convective diffusion in the adsorbate solution. It is assumed that the external resistance to mass transfer surrounding the particles is significant only in the early stages of adsorption. This is represented by the first sharper portion. The second

linear portion is the gradual adsorption stage with intra-particle diffusion dominating.

Figs.4.3.5 represent plots of q_t versus $t^{1/2}$ for the adsorption of Se(IV) onto $FeCl_3$ coated BFA, RHA, GAC and PAC. For all the systems with C_0=100 μg/l the data points represent bi-linear plots for the experimental data. The diffusion in the meso- and micro-pores is represented by the bi-linear plots for all systems shown in Fig 4.3.5. The values of I (Table 4.3.1) give an idea about the thickness of the boundary layer, i.e., the larger the intercept, the greater is the boundary layer effect. The deviation of straight lines from the origin (Fig. 4.3.5) may be because of the difference between the rate of mass transfer in the initial and final stages of adsorption. Further, such deviation of straight line from the origin indicates that the pore diffusion is not the sole rate-controlling step. The values of k_{id} for C_o = 100 μg/l as obtained from the slopes of the straight lines are listed in Table 4.3.1.

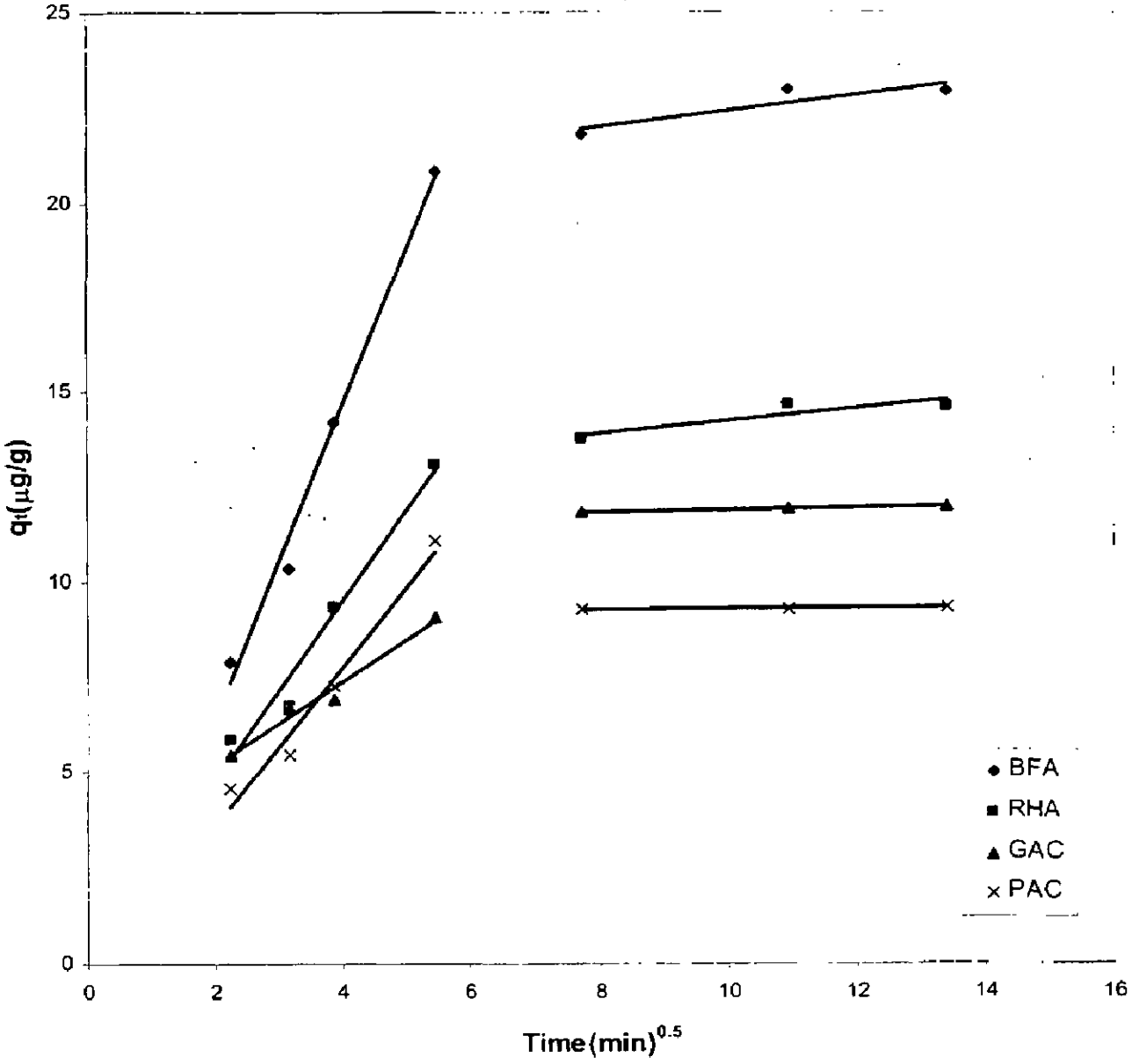

Fig. 4.3.5. Intra-particle kinetic model for the adsorption of Se(IV) at natural *pH*, optimum dosage and T = 303 K

Table 4.3.1. Kinetic parameters for the removal of Se(IV) by $FeCl_3$ coated BFA, RHA, GAC and PAC for C_0=100µg/l

	Se-BFA	Se-RHA	Se-GAC	Se-PAC
Pseudo 1st order equation	$q_t = q_e\left[1-\exp\left(-k_f t\right)\right]$			
k_f (min^{-1})	0.0540	0.0507	0.0486	0.0451
$q_{e,cal}$ (µg/g)	20.3773	11.9788	4.6471	9.4834
$q_{e,exp}$ (µg/g)	22.9700	14.6415	9.2860	11.9188
R^2	0.9857	-0.9516	-0.8968	-0.9529
Pseudo 2nd order equation	$q_t = \frac{tk_S q_e^2}{1+tk_S q_e}$			
k_s (g/µg min)	0.0056	0.0094	0.0397	0.0121
h (µg/g min)	3.2311	2.1924	3.5460	1.8795
$q_{e,cal}$ (µg/g)	24.0559	15.2674	9.4534	12.4518
R^2	0.9980	0.9984	0.9996	0.9979
Weber Morris	$q_t = k_{id} t^{1/2} + I$			
K_{id1} (µg/g min)	3.7796	2.0970	0.9141	1.5884
I_1 (µg/g)	-0.8757	0.7781	3.5373	0.8616
R^2_1	0.9779	0.9427	0.9641	0.9618
K_{id2} (µg/g min)	0.2794	0.2086	0.0236	0.0964
I_2 (µg/g)	19.4871	12.0424	9.0012	10.7576
R^2_2	0.9616	0.9616	0.7963	0.8226

4.3.6 Effect of Temperature

The effect of temperature on adsorption capacity of Se(IV) by $FeCl_3$ coated BFA, and RHA is studied by carrying out from 293 to 323 K using different initial Se(IV) concentration at natural *pH* of the solutions. The equilibrium uptake of Se(IV) by different adsorbents were affected by temperature. It was indicated that the removal increased with increase in temperature. The increase in adsorption with the rise of temperature may be due to increase in swelling of the adsorbent allowing more active sites to become available for selenium. The optimum temperature for Se(IV) adsorption on BFA and RHA was found to be the 323 K within the temperature range studied.

4.3.7 Adsorption Equilibrium Study

The experimental equilibrium adsorption data of Se(IV) adsorption onto $FeCl_3$ coated BFA, RHA, GAC and PAC have been tested by using the two-parameter Freundlich, Langmuir, and Tempkin isotherm equations.

Freundlich $$q_e = K_F C_e^{1/n} \tag{4.3.5}$$

Langmuir $$q_e = \frac{q_m K_L C_e}{1 + K_L C_e} \tag{4.3.6}$$

Tempkin $$q_e = B_T \ln K_T + B_T \ln C_e \tag{4.3.7}$$

The Freundlich isotherm is valid for a heterogeneous adsorbent surface with a non-uniform distribution of heat of adsorption over the surface. The Langmuir isotherm, however, assumes that the sorption takes place at specific homogeneous sites within the adsorbent.

The parameters of the isotherm, and the correlation coefficient, R^2 for the fitting of the experimental data are listed in Tables 4.3.2 and 4.3.3. By comparing the results of the values for the error functions (Tables 4.3.2 and 4.3.3) and correlation coefficients, it is found that the Freundlich isotherm generally represent the equilibrium sorption of Se(IV) onto BFA and RHA.

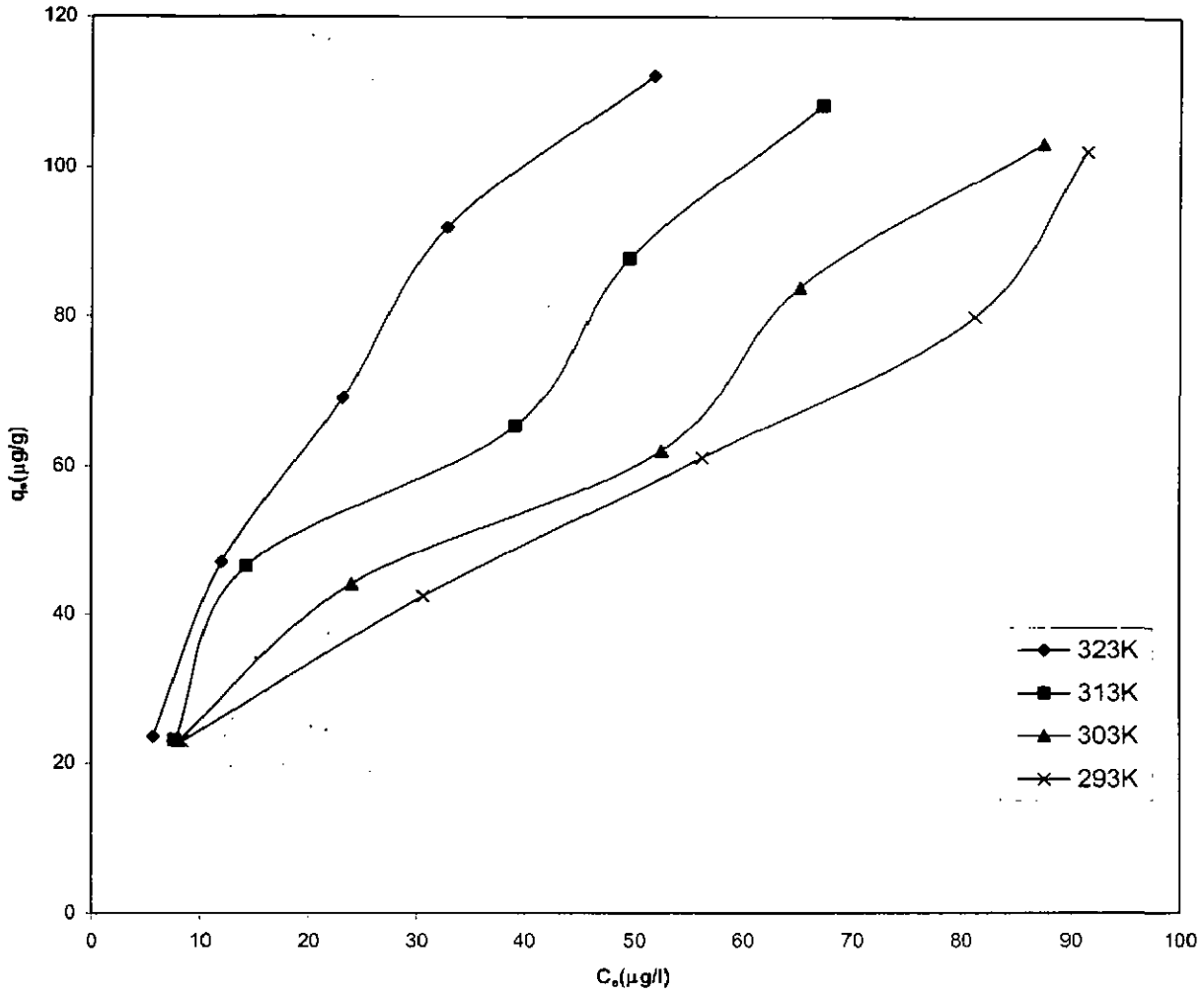

Fig 4.3.6 Equilibrium isotherms for the adsorption of Se(IV) onto BFA at different temperatures. $w = 4$ g/l, t =2 h.

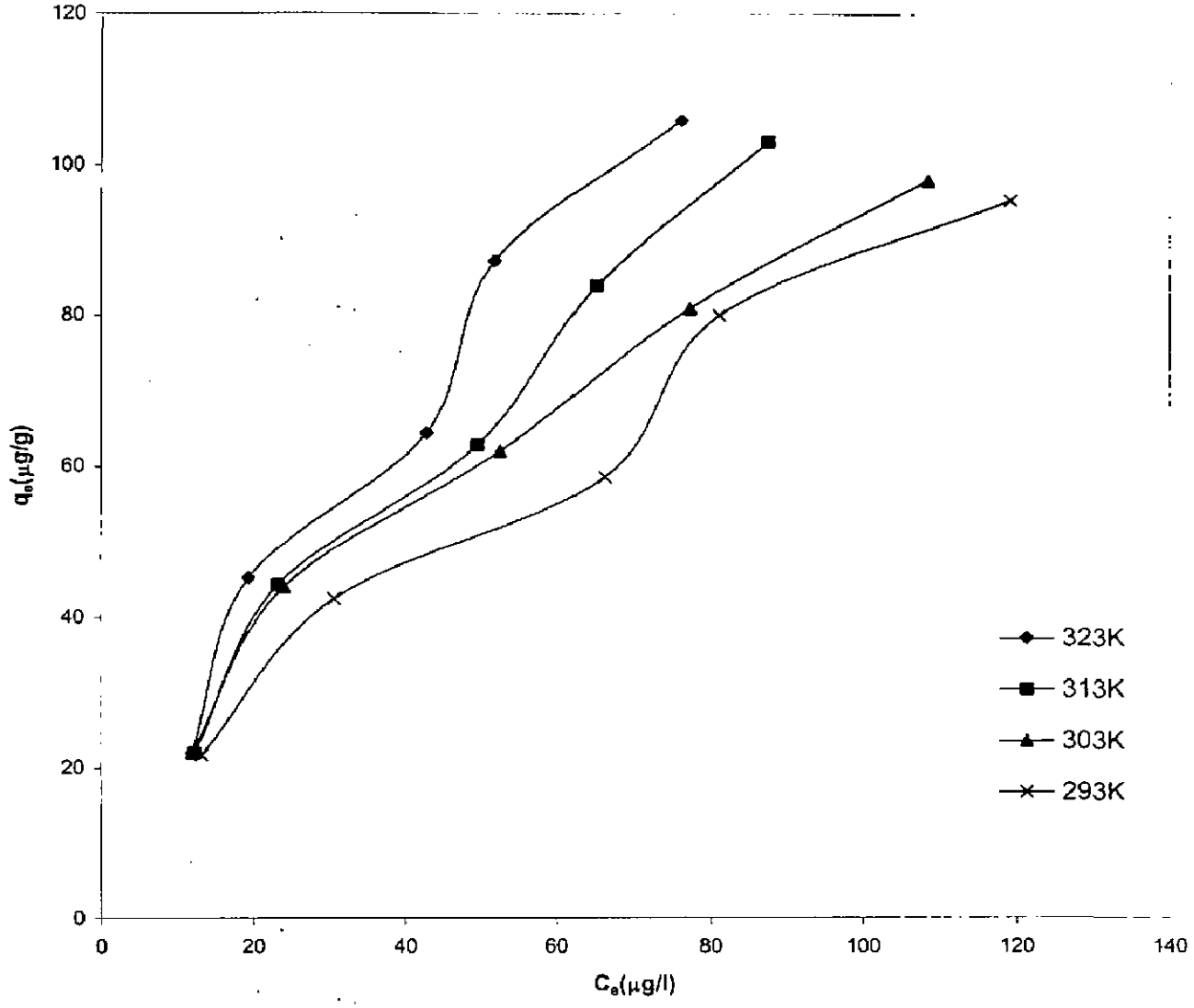

Fig 4.3.7 Equilibrium isotherms for the adsorption of Se(IV) onto RHA at different temperatures. w=6g/l, t = 2 h

Table 4.3.2. Isotherm parameters and error functions for Se(IV) adsorption onto $FeCl_3$ coated BFA

Freundlich					
Temp. (K)	K_F [(μg/g)/(μg/l)$^{1/n}$]	$1/n$	R^2	HYBRID	MPSD
293	7.32455	0.71007	0.9928	-0.370571	8.52893
303	6.78278	0.65138	0.9776	-1.0836	14.4137
313	6.29384	0.61016	0.9913	-0.216826	9.33234
323	6.12955	0.59063	0.9850	-0.288204	11.3426
Langmuir					
Temp. (K)	q_m (μg/g)	K_L (l/μg)	R^2	HYBRID	MPSD
293	207.7156	0.022875	0.9921	-76.2929	69.3467
303	176.2859	0.019948	0.9201	0.274561	14.6663
313	158.936	0.016722	0.9110	-0.498586	16.4655
323	152.5316	0.015085	0.8815	1.9052649	20.3556
Tempkin					
Temp. (K)	K_T (l/μg)	B_T	R^2	HYBRID	MPSD
293	0.2838152	40.2764	0.9912	2.07964	11.6855
303	0.2385522	35.4585	0.9654	-0.8721	14.3889
313	0.2114775	31.2207	0.9471	2.2857	23.2927
323	0.2018163	29.3437	0.9236	0.58134	27.5299

Table 4.3.3 Isotherm parameters and error functions for Se(IV) adsorption onto $FeCl_3$ coated RHA

Freundlich					
Temp. (K)	K_F [(μg/g)/(μg/l)$^{1/n}$]	$1/n$	R^2	HYBRID	MPSD
293	3.392	0.805	0.9763	-1.0515	15.0579
303	3.603	0.751	0.9892	-0.0549	9.6165
313	4.547	0.667	0.9893	-0.5127	9.76114
323	4.045	0.662	0.9911	-0.3507	9.03912
Langmuir					
Temp. (K)	q_m (μg/g)	K_L (l/μg)	R^2	HYBRID	MPSD
293	283.54	0.0078	0.8165	0.77600161	13.78
303	224.98	0.0091	0.9264	1.06117	9.6165
313	168.98	0.0126	0.9699	-2.8651	8.9889
323	163.26	0.0108	0.9438	0.30968	10.845
Tempkin					
Temp. (K)	K_T (l/μg)	B_T	R^2	HYBRID	MPSD
293	0.1357	43.19	0.9791	-0.33	11.926
303	0.13258	38.92	0.9774	0.9499	13.072
313	0.14831	33.97	0.9831	1.4138	10.506
323	0.13037	32.34	0.9698	1.3579	16.379

4.4 THERMAL DEGRADATION OF SPENT ADSORBENTS

The spent adsorbents pose problems to their disposal and management. The recent trend emphasizes on utilizing them for some beneficial purpose and rendering them innocuous and benign to the environment before they are being disposed off. The use of low-cost adsorbents for the treatment of various wastewaters generates large volumes of solid waste. These solid wastes have great potential for energy recovery. However, the separation of the adsorbents from the solvents by sedimentation, filtration, centrifugation, dewatering and drying is very important [Kumar, 2007]. Se(IV) loaded adsorbents and blank adsorbents are studied for their thermal degradation characteristics by thermogravimetric(TG) instrument.

4.4.1 Results of TGA, DTA and DTG

Thermal stability of PAC, GAC, BFA and RHA is directly dependent on the decomposition temperature of its various oxides and functional groups. The surface groups present on carbons and those formed as a result of interaction with oxidizing gases or solutions are generally quite stable even under vacuum at temperatures below 150 $^{\circ}C$, irrespective of the temperature at which they were formed. However, when the carbons are heated at higher temperatures, the surface groups decompose, producing CO (150-600 $^{\circ}C$), CO_2 (350-1000 $^{\circ}C$), water vapour and free hydrogen (500-1000 $^{\circ}C$) [Kumar, 2007]. The principal experimental variables which could affect the thermal degradation characteristics in air and nitrogen flow in a TG experiment are the pressure, the air (purge gas) flow rate, the heating rate and the weight of sample. In the present study, the operating pressure was kept slightly positive, the purge gas (air) and (nitrogen) flow rate was maintained at 200 ml/min and the heating rate was maintained at 25 K/min.

The thermogravimetric analysis (TGA), differential thermal analysis (DTA) and differential thermo gravimetery (DTG) curves of the $FeCl_3$ coated and Se(IV) adsorbed PAC.GAC, BFA and RHA are shown in Figs. 4.4.1 through 4.4.4, respectively. Three different zones can be seen in Figs. 4.4.1 and 4.4.2 for the oxidizing atmosphere for all the blank and loaded adsorbent. For PAC (Fig. 4.4.1 (a)), the first zone ranges room temperature to 400 $^{\circ}C$, the second zone from 400 $^{\circ}C$ to 870 $^{\circ}C$, and the third zone from 870 $^{\circ}C$ to 1000 $^{\circ}C$. The maximum weight loss of 78.9% was recorded in the second zone, while the first zone corresponds to comparatively much smaller weight loss of

~18%. The third zone shows almost no weight loss (~0.44%) and, therefore, no degradation. Under oxidizing atmosphere, the first zone corresponds to removal of moisture and light volatiles. The active pyrolysis and degradation zone follow this initial zone and show maximum degradation. The weight loss has been reported to be associated in part with the evolution of H_2O, CO_2 and CO. The second zone for PAC is smaller than GAC with the maximum rate of weight loss for PAC being 3.84 mg/min, 3.482 mg/min for GAC, 2.223 mg/min for BFA. and 1.79 mg/min for RHA. Subsequently, the sample weight remains almost constant in the third zone with the ash remaining at $1000\,^{\circ}C$. Thermal degradation characteristics in flowing nitrogen atmosphere show the removal of moisture of ~16.6% and 12% at a temperature of 150 $^{\circ}C$, for PAC and GAC, respectively. Thereafter, the rate of weight loss as exemplified by the DTG curve remains almost constant up to ~300 $^{\circ}C$ (weight loss of ~3% only) for PAC and GAC. For BFA (Fig. 6.6.6 (a)), a sudden increase in the rate of weight loss is observed at ~557 °C with the maximum rate being 0.375 mg/min. After 900 $^{\circ}C$, the rate of weight loss remains constant and the maximum weight loss is found to be ~3 %. This means, that the internal structure of BFA undergoes transformations under nitrogen atmosphere with the release of decomposed matter in the gaseous form.

Under oxygen atmosphere (Fig.4.4.1), three distinct zones could be seen for PAC. Below 150 $^{\circ}C$, physisorbed water removal is seen, as exemplified by the DTG and differential thermal analysis (DTA) peaks and the weight loss gradient up to $150\,^{\circ}C$ in TG curves. At temperatures larger than $400\,^{\circ}C$, degradation of PAC is seen with DTG peaks appearing at 445 $^{\circ}C$ for PAC and $485\,^{\circ}C$ for Se loaded PAC,. The DTG band is broad over a temperature range of 400-870 $^{\circ}C$. DTA broad peaks and TG weight loss curves in this temperature range support this inference. The carbon degradation is exothermic and releases energy: 3796 J/g for PAC, 3659 J/g for Se(IV) loaded GAC.

To investigate the mechanism of Se(IV) adsorption as well as the role of porosity, the nature of interaction between Se(IV) and PAC was explored by thermo-gravimetric (TG) analysis under nitrogen and air atmospheres at a heating rate of 25 K/min. A peak in derivative thermogravimetric (DTG) curve at temperature lower than 150 $^{\circ}C$ (130-$133\,^{\circ}C$) under both nitrogen and air atmospheres shows the removal of physisorbed

water. Under nitrogen atmosphere, a somewhat steady weight loss with temperature is seen in TG curve.

The TG traces for the blank and Se(IV) loaded adsorbents (Fig. 4.4.1 through 4.4.4) show that the loss of moisture and the evolution of some lightweight molecules including water take place (6.62-16.1% weight loss in air atmosphere and 5.53 -17.83 weight loss in nitrogen atmosphere) from ambient temperature to <200 $^{\circ}C$, for all the adsorbents. Higher temperature drying (> 100 $^{\circ}C$) occurs due to loss of the surface tension bound water of the particles. TG trace was also obtained for all the adsorbents, in which moisture and light volatile components loss (~31.03to 99.93% weight loss in air atmosphere and ~16.42 to 64.31% in the nitrogen atmosphere) takes place upto ~700 $^{\circ}C$ for air and ~1000 $^{\circ}C$ for nitrogen atmosphere. The distribution of volatiles released during thermal degradation and their characteristics along with DTA for blank and loaded adsorbents in an air and nitrogen atmosphere at a flow rate of 200 ml/min are presented in Tables 4.4.1 through 4.4.3.

Adsorbents (blank and loaded) show endothermic transition between room temperature and 200 $^{\circ}C$ in the air and nitrogen atmosphere, indicating phase change during the heating process. The strong exothermic peak centered between 400-700 $^{\circ}C$ is due to the oxidative degradation of the sample. This broad peak as that observed from the first derivative loss curve (DTG) as shown in Figs. 4.4.1 through Fig. 4.4.4 may be due to the combustion of carbon species. At higher temperatures (third zone), the samples present a gradual weight loss up to 950 $^{\circ}C$. This weight loss has been reported to be associated in part with the evolution of CO_2 and CO.

The maximum rate of weight loss in air atmosphere were obtained as 3.84,1.872, 2.223 and 1.79 mg/min and in the nitrogen atmosphere 1.567, 1.478,0.374 and 0.347 for PAC, GAC, BFA and RHA respectively.The nature of the TG curve gives a clear indication that the three-step degradation takes place for PAC and GAC whereas two-step degradation is observed for BFA and RHA.

Table 4.4.1 Distribution of volatiles released during thermal degradation of blank and loaded adsorbents in an air and nitrogen atmosphere at a flow rate of 200 ml/min.

Adsorbent (Blank/ loaded)	%Weight loss in air atmosphere (approximate)				%Weight loss in nitrogen atmosphere (approximate)		%Total volatile matter including moisture in air	%Total volatile matter including moisture in nitrogen
	<200 °C	200-400 °C	400-700 °C	>700 °C	<200 °C	200-1000 °C		
PAC	16.1	2.15	56.79	22.1	17.83	17.86	97.14	64.31
Se- PAC	14.93	3.1	65.94	15.96	14.31	18.57	99.93	32.88
GAC	11.78	0.65	22.51	49.44	12.5	10.77	84.38	23.27
Se- GAC	14.04	1.35	24.05	44.4	15	12.98	83.44	27.98
BFA	13.5	18.35	51.35	2.54	12.34	41.6	85.74	53.94
Se-BFA	9.03	5.9	71.7	1.75	8.31	30.72	88.38	39.03
RHA	5.97	8	15.23	1.83	6.82	13.8	31.03	20.62
Se-RHA(Fe)	6.62	2.94	20.41	1.11	5.53	10.89	31.08	16.42

Table 4.4.2 Thermal degradation characteristics of blank and loaded adsorbents in air and nitrogen atmosphere at a flow rate of 200 ml/min

Adsorbent (Blank/loaded)	Air atmosphere					Nitrogen atmosphere				
	Drying Range (^{o}C)	Moisture (%)	Degradation Range (^{o}C)	T_{max} (^{o}C)	Max. Rate of Weight Loss (mg/min)	Drying Range (^{o}C)	Moisture (%)	Degradation Range (^{o}C)	T_{max} (^{o}C)	Max. Rate of Weight Loss (mg/min)
PAC	26-190	15.1	>200	445	3.84	25-180	16.63	>200	121	1.567
Se-PAC	26-180	13.9	>200	485	3.482	24-200	13.9	>200	119	1.31
GAC	26-195	11.7	>200	667	1.872	24-200	12.46	>200	155	1.478
Se-GAC	28-190	13.1	>200	763	1.808	26-160	14.17	>200	130	1.656
BFA	26-180	12.5	>200	414	2.223	25-150	6.71	>100	557	0.374
Se-BFA	28-150	8.6	>200	463	2.576	26-180	5.8	>100	92	0.329
RHA	23-200	17.1	>200	431	1.79	26-200	3.31	>100	109	0.351
Se-RHA	28-195	2.9	>200	556	1.326	27-190	2.87	>200	103	0.357

Table 4.4.3 DTA for the blank and loaded adsorbents in the air and nitrogen atmosphere at flow rate 200 ml/min

Adsorbent (Blank/loaded)	Air atmosphere						Nitrogen atmosphere		
	ΔH_1 (MJ/kg)	T_1i (^oC)	T_2f (^oC)	ΔH_2 (MJ/kg)	T_1i (^oC)	T_2f (^oC)	ΔH (MJ/kg)	T_1i (^oC)	T_2f (^oC)
PAC	-	-	-	-3976	390	890	250	40	250
Se(IV)-PAC	152	80	200	-3659	420	850	243	25	240
GAC	118	100	220	-1203	430	880	219	24	290
Se(IV)-GAC	238	80	250	-1016	450	780	209	26	250
BFA	-	-	-	-5488	400	660	-	-	-
Se(IV)-BFA	-	-	-	-4860	400	730	-	-	-
RHA	-	-	-	-1363	400	640	-	-	-
Se(IV)-RHA	-	-	-	-1419	410	760	-	-	-

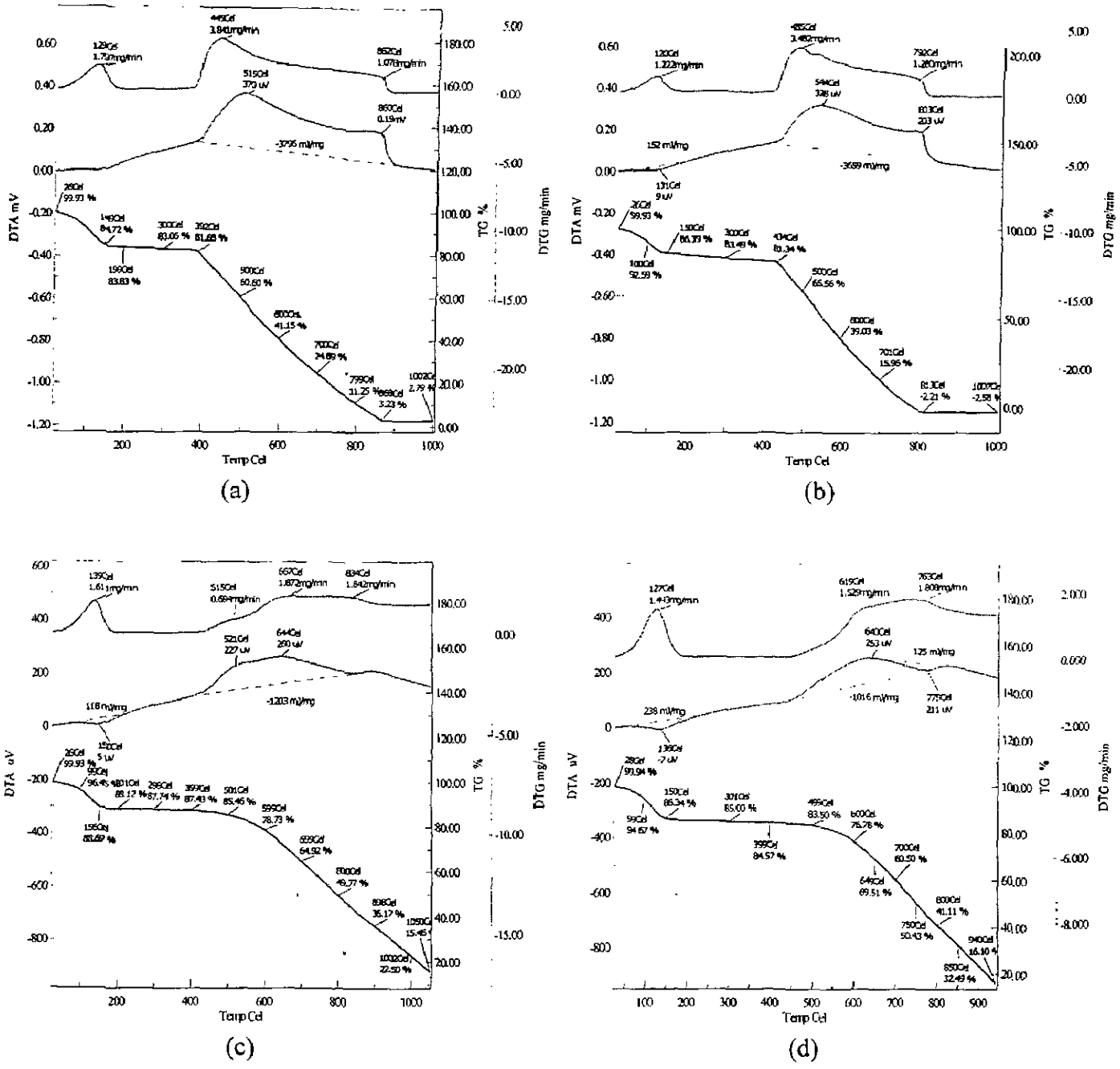

Fig:4.4.1. TGA analysis of (a) virgin and (b) Se(IV) loaded PAC($FeCl_3$);(c) virgin and (d) Se(IV) loaded GAC($FeCl_3$) in air atmosphere

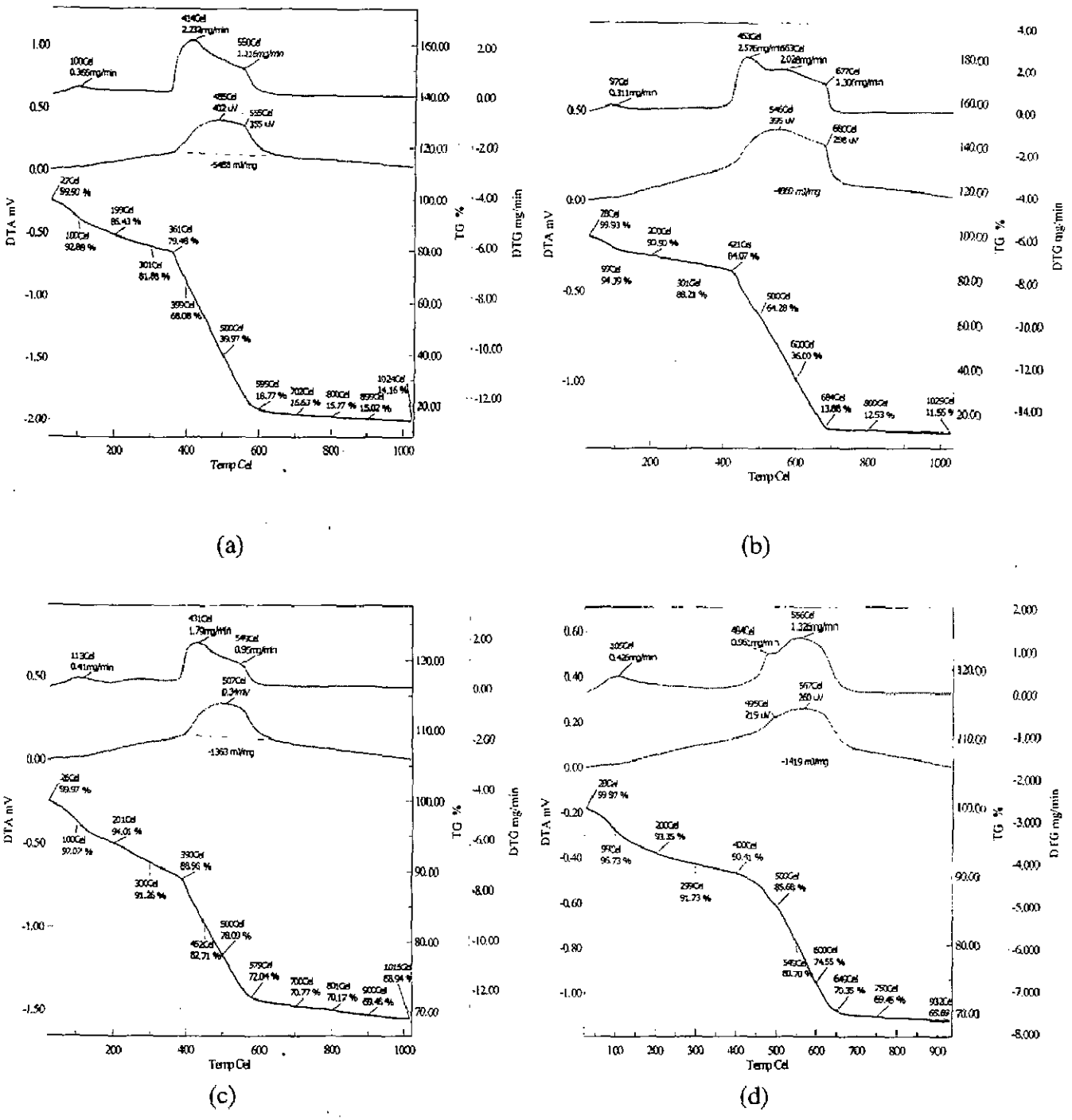

Fig:4.4.2. TGA analysis of (a) virgin and (b) Se(IV) loaded BFA ($FeCl_3$); (c) virgin and (d) Se(IV) loaded RHA($FeCl_3$) in air atmosphere

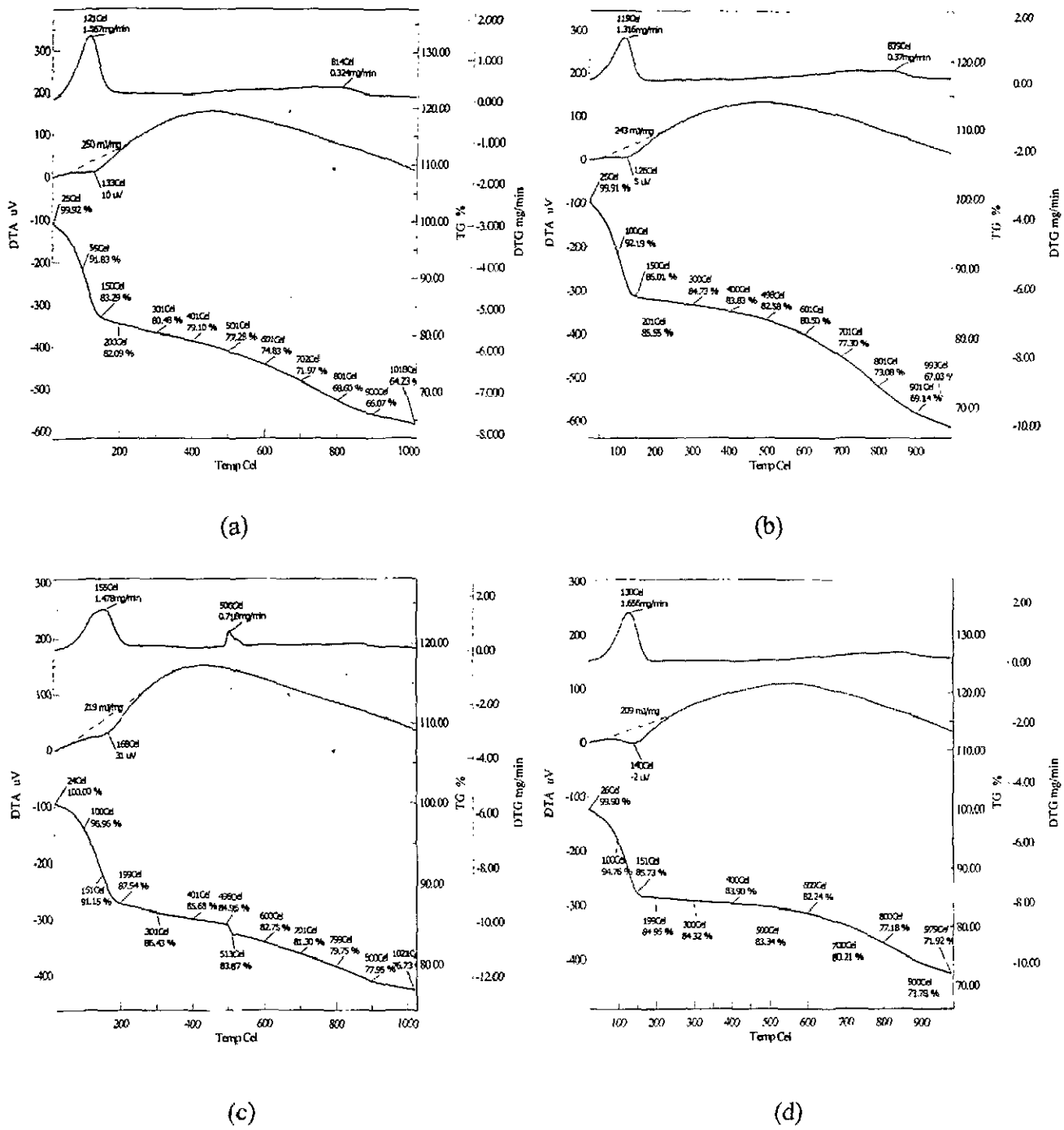

Fig:4.4.3. TGA analysis of (a) virgin and (b) Se(IV) loaded PAC($FeCl_3$);(c) virgin and (d) Se(IV) loaded GAC($FeCl_3$) in nitrogen atmosphere

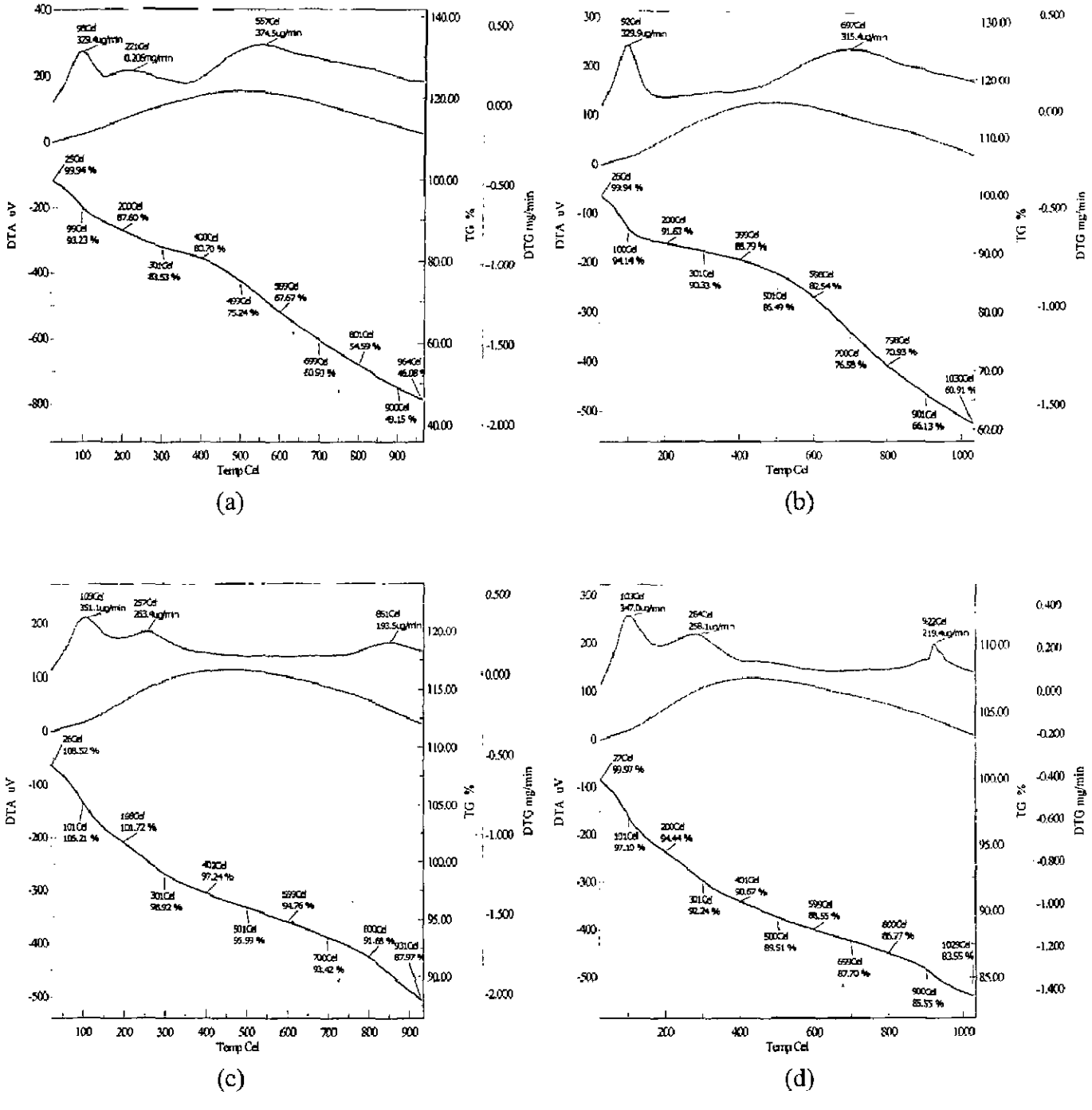

Fig:4.4.4. TGA analysis of (a) virgin and (b) Se(IV) loaded BFA ($FeCl_3$);(c) virgin and (d) Se(IV) loaded RHA($FeCl_3$) in nitrogen atmosphere

Chapter – V

CONCLUSIONS AND RECOMMENDATIONS

5.1 CONCLUSIONS

On the basis of the studies and the results and discussion presented, the following conclusions can be drawn

1 The FTIR spectra of the BFA, RHA, GAC and PAC indicated the presence of various types of functional groups e.g. free and hydrogen bonded OH group, the silanol groups (Si-OH), alkenes, CO group stretching from aldehydes and ketones on the surface of adsorbents.

2 Optimum BFA dosage is found to be 4 g/l for C_0 =100 mg/l of Se(IV) removal, whereas, optimum RHA, GAC and PAC dosage are 6, 10 and 8 g/l, respectively

3 Percent removal of Se(IV) increases with the increase in adsorbent concentration, while removal per unit weight of adsorbent increases with the decrease in adsorbent concentration.

4 Se(IV) adsorption onto all the adsorbents viz. BFA, RHA, GAC and PAC is high at low *pH* values, and decreased with the rise in initial *pH*

5 The sorption kinetics of Se(IV) onto BFA, RHA, GAC and PAC could be represented by the pseudo-second-order kinetic model.

6 The adsorption processes could be well described by a two-stage diffusion model.

7 Freundlich isotherms generally well represent the equilibrium adsorption of Se(IV) onto BFA and RHA.

5.2 RECOMMENDATIONS

On the basis of the present studies, the following recommendations may be made for future studies

1. Sale-up Column studies should be conducted to evaluate the suitability of BFA, RHA, GAC and PAC as adsorbents for the removal of Se(IV) from water. Based on column studies, actual field application may be undertaken.
2. Removal of selenium from soil may be studied.

REFERENCES

Akihiro, O.; Takuji,K.; Takashi, H.; Shiro, M. Adsorption processes of Se on the GaAs (111) A– (2x2) surface. *Applied Surface Science.* **2000,** 162-163, 419-424.

Akhtar, M.; Hasany, S. M.; Bhanger, M. I.; Iqbal, S. Low cost sorbents for the removal of methyl parathion pesticide from aqueous solutions. *Chemosphere.* **2007**, 66, 1829–1838.

Areerachakul, N.; Vigneswaran, S.; Ngo, H. H.; Kandasamy, J. Granular activated carbon (GAC) adsorption-photocatalysis hybrid system in the removal of herbicide from water. *Purif. Technol.* **2007**, 55, 214-219

Arslanoglu, F. N.; Kar, F.; Arslan, N. Adsorption of dark coloured compounds from peach pulp by using powdered-activated carbon. *J. Food. Eng.* **2005**, 71, 156–163.

Camara, C.;. Cobo, M.G.; Palacios, M.A. Selenium speciation analyses in water and sediment matrices. Quality Assurance for Environmental Analysis. *Quevauviller.* **1995.**

Derek, P. Adsorption mechanisms of selenium oxyanions at the aluminum oxide/water interface. *Colloid and Interface Science*. **2006,** 303, 337-345.

Dhillon, K.S.; Dhillon, S.K. Adsorption–desorption reactions of selenium in some soils of India. *Geoderma,***1999,** 93, 19-31.

Diban, N.; Ruiz, G.; Urtiaga, A.; Ortiz, I. Granular activated carbon for the recovery of the main peararoma compound: Viability and kinetic modelling of ethyl-2, 4-decadienoate adsorption. *J. Food. Eng.* **2007**, 78, 1259-1266.

Kumar, A. Removal of acrylonitrile and acrylic acid from aqueous solution using adsorption. *Ph.D. Thesis,***2007**

Lataye, D.H.; Mishra, I.M.; Mall, I.D. Pyridine sorption from aqueous solution by rice husk ash (RHA) and granular activated carbon (GAC): Parametric, kinetic, equilibrium and thermodynamic aspects. *J. Hazardous Materials.* **2008,** 154, 858–870.

Laurie, S.B.; Chao, T.T.;Adsorption of selenium by amorphous iron oxyhydroxide and manganese dioxide ,*Geochimica Acta,* **1990,** 54, 739-751.

Lee, J. W.; Yang, T. H.; Shim, W. G.; Kwon, T. O.; Moon, I. S. Equilibria and dynamics of liquid-phase trinitrotoluene adsorption on granular activated carbon: Effect of temperature and pH. *J. Hazard. Mater.* **2007**, 141, 185–192.

Lee, K. M.; Lim, P. E. Bioregeneration of powdered activated carbon in the treatment of alkyl-substituted phenolic compounds in simultaneous adsorption and biodegradation processes. *Chemosphere.* **2005**, 58, 407–41.

Mall, I. D.; Srivastava, V. C.; Agarwal, N. K. Adsorptive removal of Auramine-O: Kinetic and equilibrium study. *J. Hazard. Mater.* **2007**, 143(1-2), 386-395.

Mall, I. D.; Srivastava, V. C.; Agarwal, N. K.; Mishra, I. M. Adsorptive removal of malachite green dye from aqueous solution by bagasse fly ash and activated carbon- kinetic study and equilibrium isotherm analyses. *Colloids. Surfaces. A.* **2005**, 264, 17-28.

Miquel, R.; Javier, G. Sorption of selenium(IV) and selenium(VI) onto natural iron oxides: Goethite and hematite. *J. Hazardous Materials.* **2008,** 150, 279–284.

Rivera-Utrilla, J.; Mendez-Diaz, J.; Sanchez-Polo, M.; Ferro-Garcia, M.A.; Bautista-Toledo, I. Removal of the surfactant sodium dodecylbenzenesulphonate from water by simultaneous use of ozone and powdered activated carbon: Comparison with systems based on O_3 and O_3/H_2O_2. *Water. Res.* **2006**, 40, 1717–1725.

Shafey, E.I. Removal of Se(IV) from aqueous solution using sulphuric acid-treated peanut shell. *J. Environmental Management. 2007,* 84, 620–627.

Shafey, E.I. Sorption of Cd(II) and Se(IV) from aqueous solution using modified rice husk. *J.Hazardous Materials,* **2007,** 147, 546–555.

Sotiropoulos, A.K.; Kamaratos, M. Selenium adsorption on Cs-covered Si(100)2 x 1 surfaces. *Solid State Communications*, **2004,** 129, 637–641.

Sirianuntapiboon, S.; Ungkaprasatcha, O. Removal of Pb^{2+} and Ni^{2+} by bio-sludge in sequencing batch reactor (SBR) and granular activated carbon-SBR (GAC-SBR) systems. *Bioresource. Technol.* **2007**, 98, 2749–2757.

Srivastava, V. C.; Swamy, M. M.; Mall, I. D.; Prasad, B.; Mishra, I. M. Adsorptive removal of phenol by bagasse fly ash and activated carbon: equilibrium, kinetics and thermodynamic study. *Colloids. Surfaces. A:* **2006,** 272, 89-104

Tennant, M. F.; Mazyck, D. W. The role of surface acidity and pore size distribution in the adsorption of 2-methylisoborneol via powdered activated carbon. *Carbon.* **2007,** 45, 858–864

U.S. EPA. Selenium treartment and removal alternatives demonistration project. Mine Waste Technology Program Activitiy III, Project 20. EPA/600/R-01/077; **2001.**

Wang, J.; Sun, C. Adsorption voltammetry of selenium in the presence of phenylenediamine (*o*-PDA). *J. Electroanal. Chem.* **1990**, 291, 59-66

Wikipedia, http://en.wikipedia.org/wiki/Water, last accessed May 24, 2008

Wen-hui kuan.;Shang, L.L.; Ming K.W.; Cheng F.L. Removal of selenite (Se(IV)) and selenate (Se(VI)) by using Aluminum-Oxide-Coated sand. *Pregamon.* **1998,** 32, 915-923

Youwen, Y.; Vance, G. F.; Zhao, H. Selenium adsorption on Mg–Al and Zn–Al layered double hydroxides. *Applied Clay Science*, **2001,** 20, 13–25